



10 CFR 50.90

LR-N17-0092  
LAR H17-02  
April 28, 2017

U. S. Nuclear Regulatory Commission  
ATTN: Document Control Desk  
Washington, DC 20555-0001

Hope Creek Generating Station  
Renewed Facility Operating License No. NPF-57  
NRC Docket No. 50-354

Subject: **Supplemental Information to License Amendment Request to Amend the Hope Creek Technical Specifications (TS) to Revise and Relocate the Pressure-Temperature Limit Curves to a Pressure and Temperature Limits Report**

References: 1. PSEG letter to NRC, "License Amendment Request to Amend the Hope Creek Technical Specifications (TS) to Revise and Relocate the Pressure-Temperature Limit Curves to a Pressure and Temperature Limits Report" dated March 27, 2017 (ADAMS Accession No. ML17086A364)

In the Reference 1 letter, PSEG Nuclear LLC (PSEG) submitted a license amendment request (LAR) to Renewed Facility Operating License No. NPF-57 for Hope Creek Generating Station to revise the reactor coolant system Pressure-Temperature (P-T) Limit Curves (Figures 3.4.6.1-1, 3.4.6.1-2, and 3.4.6.1-3) and relocate them to a Pressure and Temperature Limits Report (PTLR).

In support of the LAR, PSEG is submitting the Hope Creek Nuclear Generating Station Unit 1 Reactor Pressure Vessel Fluence Evaluation at End of Cycle 19 with Projection to 56 EFPY report prepared by TransWare, dated March 30, 2016, as Enclosure 1.

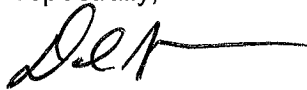
PSEG has determined that the information provided in this submittal does not alter the conclusions reached in the 10 CFR 50.92 no significant hazards determination previously submitted. In addition, the information provided in this submittal does not affect the bases for concluding that neither an environmental impact statement nor an environmental assessment needs to be prepared in connection with the proposed amendment.

There are no regulatory commitments contained in this letter. If you have any questions or require additional information, please contact Ms. Tanya Timberman at 856-339-1426.

I declare under penalty of perjury that the foregoing is true and correct.

Executed on April 28, 2018  
(Date)

Respectfully,



David J. Mannai  
Senior Director, Regulatory Operations

Enclosure:

1. TransWare Report No. EPR-HC1-001-R-002, dated March 30, 2016

cc: Administrator, Region I, NRC  
Project Manager, NRC  
NRC Senior Resident Inspector, Hope Creek  
Mr. P. Mulligan, Chief, NJBNE  
PSEG Corporate Commitment Tracking Coordinator  
Hope Creek Commitment Tracking Coordinator

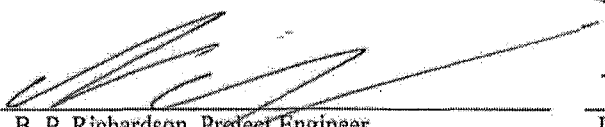
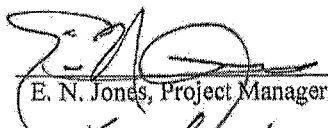
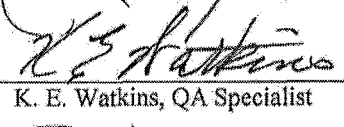
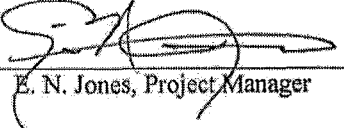
**Enclosure 1**

**TransWare Report No. EPR-HC1-001-R-002, dated March 30, 2016**

# HOPE CREEK NUCLEAR GENERATING STATION UNIT 1 REACTOR PRESSURE VESSEL FLUENCE EVALUATION AT END OF CYCLE 19 WITH PROJECTIONS TO 56 EFY

**Document Number:** EPR-HC1-001-R-002  
Revision 0

**Preparing Organization:**  
TransWare Enterprises Inc.  
1565 Mediterranean Drive  
Sycamore, IL 60178

<b>Prepared By:</b>	 _____ B. P. Richardson, Project Engineer	3-30-16 _____ Date
<b>Reviewed By:</b>	 _____ E. N. Jones, Project Manager	3/30/2016 _____ Date
<b>Reviewed By:</b>	 _____ K. E. Watkins, QA Specialist	3/30/16 _____ Date
<b>Approved By:</b>	 _____ E. N. Jones, Project Manager	3/30/2016 _____ Date

**Prepared For:**  
PSEG Nuclear LLC  
P. O. Box 236  
Hancocks Bridge, NJ 08038

and

Electric Power Research Institute, Inc.  
3420 Hillview Avenue  
Palo Alto, California 94304

EPRI Agreement No. MA 10003384NQA

Nathan A. Palm, Project Manager

Controlled Copy Number: \_\_\_\_\_

## **DISCLAIMER OF WARRANTIES AND LIMITATIONS OF LIABILITIES**

THE INFORMATION CONTAINED IN THIS REPORT IS BELIEVED BY TRANSWARE ENTERPRISES INC. TO BE AN ACCURATE AND TRUE REPRESENTATION OF THE FACTS KNOWN, OBTAINED OR PROVIDED TO TRANSWARE ENTERPRISES INC. AT THE TIME THIS REPORT WAS PREPARED. THE USE OF THIS INFORMATION BY ANYONE OTHER THAN THE CUSTOMER OR FOR ANY PURPOSE OTHER THAN FOR WHICH IT IS INTENDED, IS NOT AUTHORIZED; AND WITH RESPECT TO ANY UNAUTHORIZED USE, TRANSWARE ENTERPRISES INC. MAKES NO REPRESENTATION OR WARRANTY AND ASSUMED NO LIABILITY AS TO THE COMPLETENESS, ACCURACY OR USEFULNESS OF THE INFORMATION CONTAINED IN THIS DOCUMENT. IN NO EVENT SHALL TRANSWARE ENTERPRISES INC. BE LIABLE FOR ANY LOSS OF PROFIT OR ANY OTHER COMMERCIAL DAMAGE, INCLUDING BUT NOT LIMITED TO SPECIAL, CONSEQUENTIAL OR OTHER DAMAGES.

## **QUALITY REQUIREMENTS**

THIS DOCUMENT HAS BEEN PREPARED IN ACCORDANCE WITH THE REQUIREMENTS OF 10CFR50 APPENDIX B, 10CFR21, AND TRANSWARE ENTERPRISES INC.'S 10CFR50 APPENDIX B QUALITY ASSURANCE PROGRAM.

## **ACKNOWLEDGMENTS**

The undersigned wishes to acknowledge Mario Mazzuca and Frank Safin for their support in providing mechanical design and operating data for this fluence evaluation.

Eric N. Jones, TransWare Enterprises Inc.

# CONTENTS

<b>1</b>	<b>Introduction .....</b>	<b>1-1</b>
<b>2</b>	<b>Summary of Results.....</b>	<b>2-1</b>
<b>3</b>	<b>Description of the Reactor System .....</b>	<b>3-1</b>
3.1	Overview of the Reactor System Design.....	3-1
3.2	Reactor System Mechanical Design Inputs.....	3-2
3.3	Reactor System Material Compositions .....	3-3
3.4	Reactor Operating Data Inputs .....	3-5
3.4.1	Core Loading .....	3-5
3.4.2	Power History Data .....	3-5
3.4.3	Reactor State Point Data .....	3-8
3.4.3.1	Beginning of Operation through Cycle 19 State-points.....	3-8
3.4.3.2	Projected Reactor Operation.....	3-8
3.4.3.3	Limitation of Fluence Projections .....	3-9
<b>4</b>	<b>Calculation Methodology.....</b>	<b>4-1</b>
4.1	Description of the RAMA Fluence Methodology .....	4-1
4.2	The RAMA Geometry Model for the HC1 Reactor.....	4-2
4.2.1	The Geometry Model .....	4-5
4.2.2	The Reactor Core and Core Reflector Models .....	4-6
4.2.3	The Core Shroud Model.....	4-7
4.2.4	The Downcomer Region Model.....	4-7
4.2.5	The Jet Pump Model.....	4-7
4.2.6	The Surveillance Capsule Model.....	4-8
4.2.7	The Reactor Pressure Vessel Model.....	4-8
4.2.8	The Vessel Insulation Model .....	4-9
4.2.9	The Inner and Outer Cavity Models.....	4-9
4.2.10	The Biological Shield Model.....	4-9
4.2.11	The Above-Core Component Models .....	4-9
4.2.11.1	The Top Guide Model .....	4-9
4.2.11.2	The Core Spray Sparger Model .....	4-9
4.2.12	The Below-Core Component Models .....	4-10
4.2.13	Summary of the Geometry Modeling Approach.....	4-10
4.3	RAMA Calculation Parameters .....	4-11
4.4	RAMA Neutron Source Calculation .....	4-11
4.5	RAMA Fission Spectra.....	4-11
<b>5</b>	<b>Surveillance Capsule Activation and Fluence Results .....</b>	<b>5-1</b>
5.1	Comparison of Predicted Activation to Plant-Specific Measurements .....	5-2
5.1.1	Cycle 1 30-Degree Flux Wire Holder Activation Analysis .....	5-2

- 5.1.2 Cycle 5 30-Degree Surveillance Capsule Activation Analysis.....5-3
- 5.1.3 Cycle 19 120-Degree Surveillance Capsule Activation Analysis.....5-5
- 5.1.4 Surveillance Capsule Activation Analysis Summary.....5-8
- 5.2 Comparison of Predicted Activation to All BWR Plant Measurements.....5-9
- 6 Reactor Pressure Vessel Fluence Uncertainty Analysis .....6-1**
  - 6.1 Comparison Uncertainty .....6-1
    - 6.1.1 Operating Reactor Comparison Uncertainty.....6-2
    - 6.1.2 Benchmark Comparison Uncertainty.....6-2
  - 6.2 Analytic Uncertainty .....6-2
  - 6.3 Combined Uncertainty .....6-2
- 7 Calculated Reactor Pressure Vessel Neutron Fluence for Energy >1.0 MeV .....7-1**
- 8 References.....8-1**

## LIST OF FIGURES

Figure 3-1	Planar View of HC1 at the Core Mid-Plane Elevation.....	3-2
Figure 3-2	Projection Cycle Relative Power Map (PANAC Fuel Coordinates).....	3-10
Figure 3-3	Projection Cycle Average Nodal Relative Power Axial Profile (Core Periphery) .....	3-11
Figure 4-1	Planar View of the HC1 RAMA Quadrant Model at the Core Mid-Plane Elevation.....	4-3
Figure 4-2	Axial View of the HC1 RAMA Model.....	4-4
Figure 7-1	HC1 RPV Shell Plate, Weld and Nozzle Identifiers .....	7-2
Figure 7-2	Nozzle Edit Locations for Sample Nozzle.....	7-4

## LIST OF TABLES

Table 2-1	Maximum Fast Neutron Fluence for HC1 RPV Shell Plates at EOC 19 and 56 EFPY .....	2-1
Table 2-2	Maximum Fast Neutron Fluence for HC1 RPV Welds at EOC 19 and 56 EFPY .....	2-2
Table 2-3	RPV Beltline Elevation Range for HC1 for Energy >1.0 MeV .....	2-3
Table 3-1	Summary of Material Compositions by Region for HC1.....	3-4
Table 3-2	Summary of HC1 Core Loading Inventory.....	3-6
Table 3-3	State-point Data for Each Cycle of HC1 .....	3-7
Table 3-4	Projection Cycle Operating Characteristics .....	3-9
Table 5-1	Comparison of Specific Activities for the HC1 Cycle 1 Flux Wire Holder Wires (C/M).....	5-3
Table 5-2	Comparison of Specific Activities for HC1 Cycle 5 Surveillance Capsule Flux Wires Using As-Built Dimensions (C/M) .....	5-4
Table 5-3	Comparison of Specific Activities for HC1 Cycle 5 Surveillance Capsule Flux Wires Using Nominal Dimensions (C/M).....	5-5
Table 5-4	Comparison of Specific Activities for HC1 Cycle 19 Surveillance Capsule Flux Wires Using As-Built Dimensions (C/M) .....	5-7
Table 5-5	Comparison of Specific Activities for HC1 Cycle 19 Surveillance Capsule Flux Wires Using Nominal Dimensions (C/M).....	5-8
Table 5-6	Comparison of Activities for HC1 Flux Wires Using As-Built Dimensions .....	5-9
Table 5-7	Comparison of Activities for HC1 Flux Wires Using Nominal Dimensions .....	5-9
Table 5-8	Summary of BWR Operating Reactor Surveillance Capsule Measurement Comparisons.....	5-10
Table 6-1	HC1 RPV Uncertainty for Energy >1.0 MeV .....	6-3
Table 7-1	Maximum Fast Neutron Fluence for HC1 RPV Beltline Weld Locations at EOC 19 (24.1 EFPY) .....	7-5
Table 7-2	Maximum Fast Neutron Fluence for HC1 RPV Beltline Shell Plate Locations at EOC 19 (24.1 EFPY) .....	7-6
Table 7-3	Maximum Fast Neutron Fluence for HC1 RPV Beltline Nozzle Locations at EOC 19 (24.1 EFPY).....	7-6
Table 7-4	Maximum Fast Neutron Fluence for HC1 RPV Beltline Weld Locations at 56 EFPY .....	7-7
Table 7-5	Maximum Fast Neutron Fluence for HC1 RPV Beltline Shell Plate Locations at 56 EFPY .....	7-8
Table 7-6	Maximum Fast Neutron Fluence for HC1 RPV Beltline Nozzle Locations at 56 EFPY .....	7-8
Table 7-7	Reactor Beltline Elevation Range for HC1 for Energy >1.0 MeV .....	7-9

## GLOSSARY OF TERMS

**AZIMUTHAL QUADRANT SYMMETRY** – A type of core and pressure vessel configuration that can be represented by a single quadrant that can be rotated and mirrored to represent the entire 360-degree geometry. The northeast quadrant can be mirrored to represent the northwest and southeast quadrants and can be rotated to represent the southwest quadrant.

**BEST ESTIMATE NEUTRON FLUENCE** – See Neutron Fluence.

**CALCULATED NEUTRON FLUENCE** – See Neutron Fluence.

**CALCULATIONAL BIAS** – A calculational adjustment based on comparisons of calculations to measurements. If a bias is determined to exist, it may be applied as a multiplicative correction to the calculated fluence to determine the best-estimate neutron fluence.

**CORE BELTLINE** – The axial elevations corresponding to the active fuel region of the core.

**EFFECTIVE FULL POWER YEARS (EFPY)** – A unit of measurement representing one full year at the reactor’s rated power level for that time period. If the reactor operates for 10 months at full rated power, then goes into a power uprate and continues operating for another 2 months at the new full rated power, this represents 1 EFPY.

**FAST NEUTRON FLUENCE** – Fluence accumulated by neutrons with energy greater than 1.0 MeV (>1.0 MeV).

**NEUTRON FLUENCE** – Time-integrated neutron flux reported in units of n/cm<sup>2</sup>. The term “best-estimate” fluence refers to the values that are computed in accordance with the requirements of U. S. Nuclear Regulatory Commission Regulatory Guide 1.190 for use in material embrittlement evaluations. The term “calculated” fluence refers to the values that are predicted by the RAMA Fluence Methodology. In this report the best-estimate fluence is synonymous with the calculated fluence since the RAMA Fluence Methodology requires no bias correction to the calculated fluence.

**RPV** – An abbreviation for reactor pressure vessel. Unless otherwise noted, the reactor pressure vessel refers to the base metal material (i.e., excluding clad/liner).

**RPV BELTLINE** – The region of the reactor vessel (shell material, including welds, heat-affected zones, and plates or forgings) that directly surrounds the effective height of the active core and adjacent regions of the reactor vessel that are predicted to experience sufficient neutron radiation damage to be considered in the selection of the most limiting material with regard to radiation damage. For purposes of this evaluation, the adjacent regions predicted to experience sufficient

neutron radiation damage are considered to be those within the axial elevations corresponding to the regions where the RPV exceeds a fast neutron fluence of  $1.0E+17$  n/cm<sup>2</sup>.

**RPV ZERO ELEVATION** – Axial elevations cited in this report assume that RPV zero is at the inside surface of the lowest point in the vessel bottom head

# 1

## INTRODUCTION

This report presents the results of the reactor pressure vessel (RPV) fluence evaluation performed for the Hope Creek Nuclear Generating Station Unit 1 reactor (HC1). In this analysis, maximum fast neutron (energy >1.0 MeV) fluence is reported for the RPV welds, shells and nozzles within the RPV beltline region, as well as the extent of the beltline region. Fluence is calculated at the end of cycle (EOC) 19 and projected to 56 effective full power years of operation (EFPY), which is assumed to represent the end of the reactor's extended operating license.

The fluence values presented in this report were calculated using the RAMA Fluence Methodology [1]. Under funding from Electric Power Research Institute, Inc. (EPRI) and the Boiling Water Reactor Vessel and Internals Project (BWRVIP), the RAMA Fluence Methodology was developed by TransWare Enterprises Inc. for the purpose of calculating fast neutron fluence in nuclear reactor pressure vessels and vessel internal components. The RAMA Fluence Methodology (hereinafter referred to as RAMA) has been reviewed by the U. S. NRC on two separate occasions, resulting in the issuance of Safety Evaluation Reports (SERs) providing conditional approval of the RAMA methodology for determining fast neutron fluence in BWR pressure vessels [2] and vessel internal components that include the core shroud and top guide [3]. As part of the license renewal application for the Seabrook Station Nuclear Power Plant [4], the U. S. NRC performed a subsequent review of the methodology, resulting in an extended approval of the RAMA methodology, specifically noting that "the RAMA methodology is generically approved by the NRC staff for [determining pressure vessel neutron fluence in] BWRs and PWRs." The conditional approval of the RAMA methodology for determining neutron fluence in reactor internals is specifically cited in the SER [3] stating that the staff will "accept RAMA calculated fluence values for BWR core shrouds and top guide for licensing actions provided that the calculation results are supported by sufficient justification that the proposed values are conservative for the intended application."

As prescribed in Regulatory Guide 1.190 [5], TransWare Enterprises Inc. has benchmarked the RAMA Fluence Methodology against industry standard benchmarks for both boiling water reactor (BWR) and pressurized water reactor (PWR) designs, and compared with plant-specific dosimetry measurements and reported fluence from numerous commercial operating reactors. The results of the benchmarks and comparisons to measurements that TransWare has performed show that the RAMA methodology accurately predicts specimen activities in all light water reactor types. The overall comparison results determined by TransWare for 600 measurements is calculated to be  $0.99 \pm 0.09$ .

The information and associated evaluations provided in this report have been performed in accordance with the requirements of 10CFR50 Appendix B [6].

# 2

## SUMMARY OF RESULTS

This section provides a summary of the fast neutron fluence evaluation performed for the HC1 RPV. The focus of the evaluation was to determine the maximum fast neutron fluence accumulated in the RPV beltline welds, shells and nozzles. Fluence was projected to the end of the reactor's extended design life of 56 EFY.

Table 2-1 summarizes the maximum fast neutron fluence at EOC 19 and at 56 EFY for the RPV shell plates discussed in the previous paragraph and Table 2-2 summarizes the results for the RPV weld locations. The highest fluence in all shell plate locations evaluated is in the lower-intermediate shell with a value of 1.63E+18 n/cm<sup>2</sup> at 56 EFY. The highest fluence in all weld locations evaluated is in the lower-intermediate shell axial welds 14-2 and 14-3 with a value of 1.43E+18 n/cm<sup>2</sup> at 56 EFY. These values are shown in **bold** type in Table 2-1 and Table 2-2. Fluence values that exceed the threshold fluence of 1.0E+17 n/cm<sup>2</sup> are shown in **red**.

**Table 2-1**  
**Maximum Fast Neutron Fluence for HC1 RPV Shell Plates at EOC 19 and 56 EFY**

Component	Heat or Heat/Lot	Fast Neutron Fluence at 0T (n/cm <sup>2</sup> )	
		EOC 19	56 EFY
<b>Shell Plates</b>			
Intermediate Shell Plate	5K3025/1 5K2608/1 5K2698/1	<b>2.35E+17</b>	<b>5.55E+17</b>
<b>Lower-Intermediate Shell Plate</b>	<b>5K2963/1</b> <b>5K2530/1</b> <b>5K3238/1</b>	<b>6.34E+17</b>	<b>1.63E+18</b>
Lower Shell Plate	5K3230/1 6C35/1 6C45/1	<b>4.26E+17</b>	<b>1.15E+18</b>

**Table 2-2  
Maximum Fast Neutron Fluence for HC1 RPV Welds at EOC 19 and 56 EPFY**

Component	Heat or Heat/Lot	Fast Neutron Fluence at 0T (n/cm <sup>2</sup> )	
		EOC 19	56 EPFY
<b>RPV Beltline Welds</b>			
Int. Shell Axial Weld 13-1	510-01205 D53040/1125-02205	1.85E+17	4.32E+17
Int. Shell Axial Weld 13-2		2.31E+17	5.50E+17
Int. Shell Axial Weld 13-3		9.14E+16	2.16E+17
Lower-Int. Shell Axial Weld 14-1	<b>510-01205</b> <b>D53040/1125-02205</b>	2.16E+17	5.56E+17
<b>Lower-Int. Shell Axial Weld 14-2</b>		<b>5.56E+17</b>	<b>1.43E+18</b>
<b>Lower-Int. Shell Axial Weld 14-3</b>		<b>5.56E+17</b>	<b>1.43E+18</b>
Lower Shell Axial Weld 15-1	510-01205 D53040/1125-02205	3.71E+17	1.00E+18
Lower Shell Axial Weld 15-2		2.81E+17	7.00E+17
Lower Shell Axial Weld 15-3		2.71E+17	7.20E+17
Int./Lower-Int. Shell Girth Weld 6	519-01205 504-01205 510-01205 D53040/1810-02205 D55733/1810-02205	2.35E+17	5.55E+17
Lower-Int./Lower Shell Girth Weld 7	501-01205 D53040/1125-02205	4.26E+17	1.15E+18
<b>Nozzle Forging-to-Base-Metal Welds</b>			
Nozzle Weld N2	N/A	1.35E+16	3.74E+16
Nozzle Weld N16	N/A	1.51E+17	3.58E+17
Nozzle Weld N17	001-01205 519-01205 504-01205	2.09E+17	4.81E+17

The reactor beltline region, as defined in Appendices G [7] and H [8] of 10CFR50, includes the region that directly surrounds the effective height of the reactor core as well as those adjacent areas of the RPV that are predicted to experience sufficient neutron irradiation damage. As identified for the definition of the RPV beltline, this is considered to include all materials that exceed a neutron fluence ( $E > 1.0$  MeV) of  $1.0E+17$  n/cm<sup>2</sup>. The elevation ranges at which the RPV fluence exceeds  $1.0E+17$  n/cm<sup>2</sup> for the two reporting periods are given in Table 2-3. These elevations define the RPV beltline region for that time period.

**Table 2-3**  
**RPV Beltline Elevation Range for HC1 for Energy >1.0 MeV**

Reactor Lifetime	Lower Elevation [cm (in)]	Upper Elevation [cm (in)]
EOC 19 (24.1 EFPY)	541.78 (213.30)	937.92 (369.26)
56 EFPY	518.10 (203.98)	958.07 (377.19)

Section 7 contains tables of results listing the fast neutron fluence for all of the RPV circumferential (girth) welds, vertical (axial) welds, nozzles, and plates included in this evaluation at 0T, 1/4 T and 3/4 T.

Comparisons were made between the calculated and measured specific activities for three sets of surveillance capsule dosimetry specimens removed from HC1. It is noted that there is a significant difference between the calculated results for the capsules, depending on whether as-built or nominal dimensions are used for their position. The results for both configurations are presented in this report. The total average calculated-to-measured (C/M) results for HC1 dosimetry specimens using as-built dimensions is 1.10 with a standard deviation of  $\pm 0.09$ . The total average calculated-to-measured (C/M) results for HC1 dosimetry specimens using nominal dimensions is 1.00 with a standard deviation of  $\pm 0.06$ . A more detailed assessment of the surveillance capsule activation analyses is presented in Section 5 of this report.

Another result from this evaluation is the calculated RPV fluence combined uncertainty value. By combining the comparison uncertainty and analytic uncertainty, the combined RPV fast neutron fluence uncertainty is determined to be 9.9% with no bias correction to the fluence. In conclusion, it is determined that RAMA produces results that meet the requirements of U. S. NRC Regulatory Guide 1.190.

# 3

## DESCRIPTION OF THE REACTOR SYSTEM

This section provides an overview of the reactor design and operating data inputs that were used to develop the HC1 reactor fluence model. All reactor design and operating data inputs used to develop the model were plant-specific and were provided by PSEG Nuclear, LLC [9-19]. Any design drawings that have been revised since the previous evaluation, or which have additionally been provided for this evaluation, were evaluated as to their impact on the fluence model and no discrepancies were found. The inputs for the fluence geometry model were developed from design and as-built drawings for the reactor pressure vessel, vessel internals, fuel assemblies, and containment regions. Several modifications were made to the HC1 RAMA geometry model since the previous vessel fluence evaluation performed by TransWare in 2008 [20]. These modifications include:

- Adding RPV nozzle forgings including N2 (recirculation inlet) and N17 (LPCI) nozzles
- Adding jet pump repair assemblies, hold down beams and hold down brackets
- Adding core support plate rim bolts
- Improved shroud head model
- Improved below core model, including fuel support pieces and control rod guide tubes

The reactor operating data inputs were developed from core simulator data that provided a historical accounting of how the reactor operated for cycles 1 through 19 [9-12]. The operating data for cycle 18 was used to project fluence to the end of the reactor's extended operating life.

### 3.1 Overview of the Reactor System Design

HC1 is a General Electric BWR/4 class reactor with a core loading of 764 fuel assemblies. HC1 began commercial operation in 1986 with a design rated power of 3293 MWt. In cycle 10, a power up-rate was achieved, raising the power to 3339 MWt. Two power up-rates were achieved during cycle 15 to 3723 MWt, and then to 3840 MWt.

Figure 3-1 illustrates the basic planar configuration of the HC1 reactor at an axial elevation near the reactor core mid-plane. All of the radial regions of the reactor that are required for fluence projections are shown. Beginning at the center of the reactor and projecting outward, the regions include: the core region, including control rod locations and fuel assembly locations (fuel locations are shown only for the 0-to-90-degree quadrant); core reflector region (bypass water); central shroud wall; downcomer water region including the jet pumps; reactor pressure vessel (RPV) wall; cavity region between the RPV wall and insulation; insulation; cavity region between the insulation and biological shield; and biological shield (concrete wall).

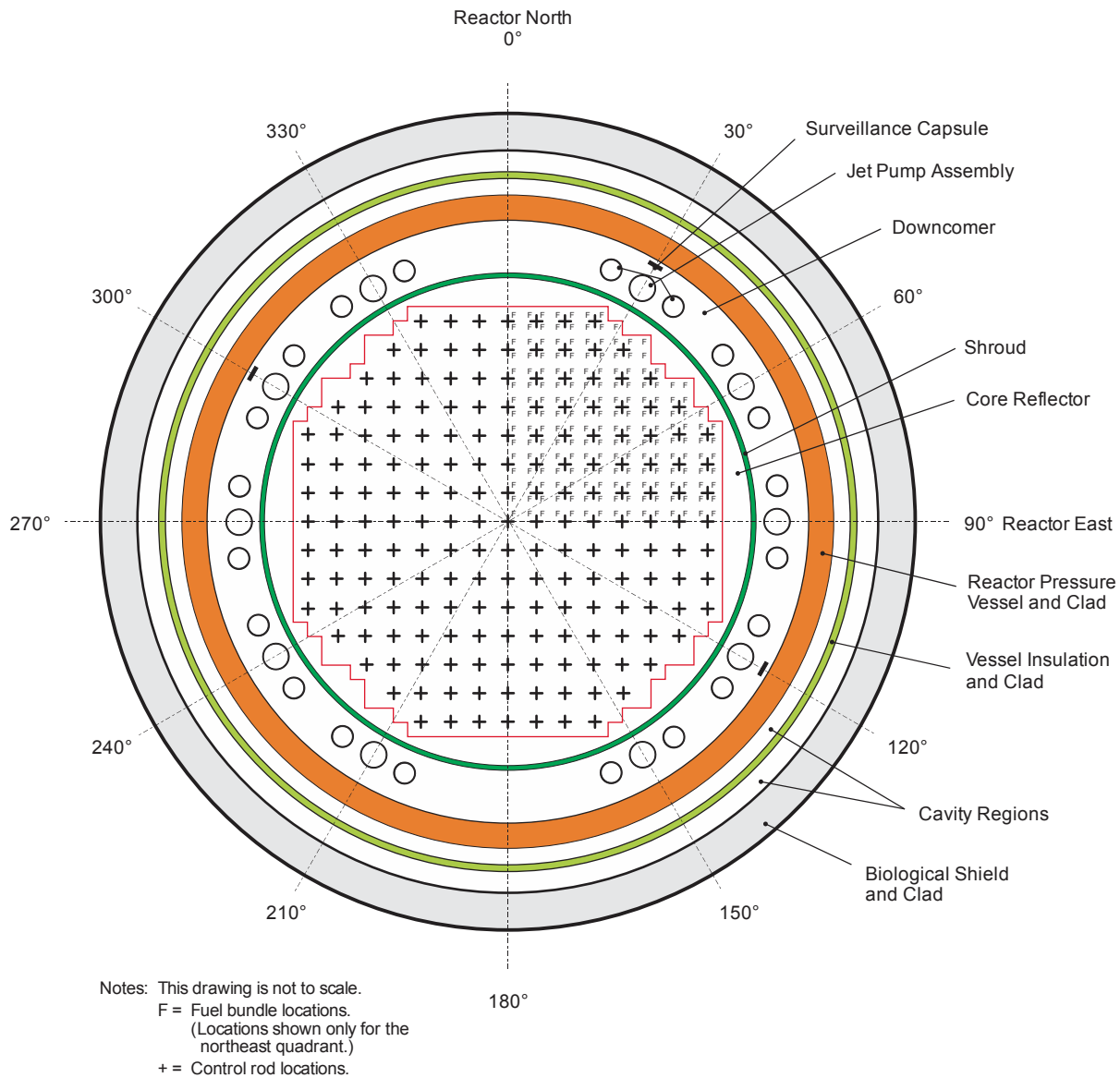


**Figure 3-1**  
**Planar View of HC1 at the Core Mid-Plane Elevation**

### 3.2 Reactor System Mechanical Design Inputs

The mechanical design inputs that were used to construct the HC1 fluence geometry model included nominal and as-built design dimensional data [17-19]. As-built data for the reactor components and regions of the reactor system is always preferred when constructing plant-specific models; however, as-built data is not always available. In these situations, nominal design information is used.

For the HC1 fluence model, the predominant dimensional information used to construct the fluence model was nominal design data. As-built data was used for the following dimensions:

- Surveillance capsule azimuthal position
- Surveillance capsule lower mounting bracket bail to RPV cladding distance

Another important component of the fluence analysis is the accurate description of the surveillance capsules in the reactor. It is shown in Figure 3-1 that three surveillance capsules were initially installed in the HC1 reactor. The capsules were attached radially to the inside surface of the RPV (looking outward from the core region) at the 30-, 120-, and 300-degree azimuths. Surveillance capsules are used to monitor the radiation accumulated in the reactor over a period of time. The importance of surveillance capsules in fluence analyses is that they contain flux wires that are irradiated during reactor operation. When a capsule is removed from the reactor, the irradiated flux wires are evaluated to obtain activity measurements. These measurements are used to validate the fluence model. Three sets of flux wires have been removed from the HC1 reactor and analyzed. An evaluation was performed comparing the calculated activities in the flux wires based on the RAMA fluence model to the activation measurements [21].

### **3.3 Reactor System Material Compositions**

Each region of the reactor is comprised of materials that include reactor fuel, steel, water, insulation, concrete, and air. Accurate material information is essential for the fluence evaluation as the material compositions determine the scattering and absorption of neutrons throughout the reactor system and, thus, affect the determination of neutron fluence in the reactor components.

Table 3-1 provides a summary of the materials for the various components and regions of the HC1 reactor. The material attributes for the steel, insulation, concrete, and air compositions (i.e. material densities and isotopic concentrations) are assumed to remain constant for the operating life of the reactor. The attributes of the fuel compositions in the reactor core region change continuously during an operating cycle due to changes in power level, fuel burnup, control rod movements, and changing moderator density levels (voids). Because of the dynamics of the fuel attributes with reactor operation, several state-point data sets are used to describe the operating states of the reactor for each operating cycle. The number of data sets used in this analysis is presented in Section 3.4.3.1.

**Table 3-1  
Summary of Material Compositions by Region for HC1**

Region	Material Composition
Control Rods	Stainless Steel, B <sub>4</sub> C
Control Rod Guide Tubes	Stainless Steel
Core Support Plate	Stainless Steel
Core Support Plate Rim Bolts	Stainless Steel
Fuel Support Piece	Stainless Steel
Fuel Assembly Lower Tie Plate	Stainless Steel, Zircaloy, Inconel
Reactor Core	<sup>235</sup> U, <sup>238</sup> U, <sup>239</sup> Pu, <sup>240</sup> Pu, <sup>241</sup> Pu, <sup>242</sup> Pu, O <sub>fuel</sub> , Zircaloy
Reactor Coolant / Moderator	Water
Core Reflector	Water
Fuel Assembly Upper Tie Plate	Stainless Steel, Zircaloy, Inconel
Top Guide	Stainless Steel
Core Spray Sparger Pipes	Stainless Steel
Core Spray Sparger Flow Areas	Steam
Shroud	Stainless Steel
Downcomer Region	Water
Jet Pump Riser and Mixer Flow Areas	Water
Jet Pump Riser and Mixer Metal	Stainless Steel
Jet Pump Riser Brace and Pads	Stainless Steel
Jet Pump Hold Down Beams	Inconel
Jet Pump Hold Down Brackets	Stainless Steel
Surveillance Capsule Specimens	Carbon Steel
Reactor Pressure Vessel Clad	Stainless Steel
Reactor Pressure Vessel Wall	Carbon Steel
RPV Nozzle Forgings	Carbon Steel
RPV Nozzle Forging Interior	Water
Cavity Regions	Air
Insulation Clad	Stainless Steel
Insulation	Glasswool
Biological Shield Clad	Carbon Steel
Biological Shield Wall	Reinforced Concrete

## **3.4 Reactor Operating Data Inputs**

An accurate evaluation of reactor vessel and component fluence requires an accurate accounting of the reactor's operating history. The primary reactor operating parameters that affect the determination of fast neutron fluence in light water reactors include reactor power levels, core power distributions, coolant water density distributions, and fuel material (isotopic) distributions.

### **3.4.1 Core Loading**

It is common in BWRs that more than one fuel assembly design may be loaded in the reactor core in any given operating cycle. For fluence evaluations, it is important to account for the fuel assembly designs that are loaded in the core in order to accurately represent the neutron source distribution at the core boundaries (i.e. peripheral fuel locations and the top and bottom fuel elevations).

Several different fuel assembly designs were loaded in the HC1 reactor during the period included in this evaluation. Table 3-2 provides a summary of the fuel designs loaded in the reactor core for these operating cycles. The cycle core loading provided by PSEG Nuclear, LLC was used to identify the fuel assembly designs in each cycle and their location in the core loading inventory. For each cycle, appropriate fuel assembly models were used to build the reactor core region of the HC1 RAMA fluence model.

### **3.4.2 Power History Data**

Reactor power history is the measure of reactor power levels and core exposure on a continual or periodic basis. For this fluence evaluation, the power history for the HC1 reactor was developed from power history inputs provided by PSEG Nuclear, LLC [9-16]. The power history data showed that HC1 started commercial operation with a design rated thermal power 3293 MWt. In cycle 10, a power up-rate was achieved, raising the power to 3339 MWt. Cycle 15 began operation at 3339 MWt, and had 2 power up-rates during the cycle to 3723 MWt and then 3840 MWt. Cycle 16 and beyond operated at 3840 MWt, and it is assumed that all cycles until the end of life will continue to operate at that power.

The power history data for HC1 included daily power levels for cycles 1 through 19. This data was used to calculate the fluence for the vessel internal components. Periods of reactor shutdown due to refueling outages and other events were also accounted for in the model. The power history data was verified by comparing the calculated energy production in effective full power years with power production records provided by PSEG Nuclear, LLC. Table 3-3 lists the accumulated EFPY at the end of each cycle for this fluence evaluation.

**Table 3-2  
Summary of HC1 Core Loading Inventory**

Cycle	8x8 Designs		10x10 Designs		Dominant Peripheral Design
	GE 7	GE 9	Westinghouse SVEA 96	GE 14	
1	764				GE 7
2	764				GE 7
3	764				GE 7
4	500	264			GE 7
5	252	512			GE 7
6	20	744			GE 9
7		764			GE 9
8		764			GE 9
9		764			GE 9
10		532	232		GE 9
11		292	472		GE 9
12		53	711		GE 9
13			600	164	SVEA 96
14			444	320	SVEA 96
15			216	548	SVEA 96
16				764	GE 14
17				764	GE 14
18				764	GE 14
19				764	GE 14
19+(1)				764	GE 14

1) Beyond cycle 19, cycle 18 data is used for projecting fluence to the end of the extended plant license period.

**Table 3-3  
State-point Data for Each Cycle of HC1**

Cycle Number	Number of State Point Data Files	Rated Thermal Power <sup>(1)</sup> (MWt)	Accumulated Effective Full Power Years (EFPY)
1	18	3293	1.0
2	15	3293	2.3
3	10	3293	3.3
4	18	3293	4.8
5	9	3293	6.0
6	12	3293	7.4
7	17	3293	8.8
8	10	3293	9.9
9	12	3293	10.9
10	18	3293, 3339 <sup>(2)</sup>	12.1
11	16	3339	13.5
12	14	3339	14.7
13	11	3339	15.7
14	15	3339	17.1
15	21	3339, 3723, 3840 <sup>(2)</sup>	18.5
16	20	3840	19.9
17	18	3840	21.3
18	20	3840	22.7
19	19	3840	24.1
19+ <sup>(3)</sup>	20	3840	56.0

- 1) The rated thermal power is listed for each cycle, however, actual power levels were used for the individual state-points calculations.
- 2) A power update to 3339 MWt was achieved during cycle 10, and to 3723 MWt and then to 3840 MWt during cycle 15.
- 3) Operating data beyond cycle 19 was not available at the time of this analysis. Cycle 18 is used as the best-estimate “equilibrium” cycle for projecting fluence to the end of the plant license.

### **3.4.3 Reactor State Point Data**

Core simulator data was provided by PSEG Nuclear, LLC to characterize the historical operating conditions of HC1 for cycles 1 through 19 [9-12]. The data calculated with core simulator codes represents the best-available information about the reactor core's operating history over the reactor's operating life. In this analysis, the core simulator data provided by PSEG was processed by TransWare to generate state-point data files for input to the RAMA fluence model. The state-point files included three-dimensional data arrays that described core power distributions, fuel exposure distributions, fuel materials (isotopes), and coolant water densities.

A separate neutron transport calculation was performed for each of the state points tallied in Table 3-3. The calculated neutron flux for each state point was combined with the appropriate power history data described in Section 3.4.2 in order to provide an accurate accounting of the fast neutron fluence for the vessel internal components. Fluence projections to the end of the reactor's extended design life were performed using cycle 18 as discussed in Section 3.4.3.2.

#### **3.4.3.1 Beginning of Operation through Cycle 19 State-points**

A total of 293 state points were used to represent the operating history for the first 19 completed operating cycles of HC1. These state points were selected from hundreds of exposure points that were calculated with the core simulator code. The hundreds of exposure points were evaluated and grouped into a fewer number of exposure ranges in order to reduce the number of transport calculations required to perform the fluence evaluation. Several criteria were used in the determination of the exposure ranges, including evaluations of core thermal powers, core flows, core power profiles, and control rod patterns. In determining exposure ranges, it is assumed that there will be at least one exposure step in that range that would accurately represent the average operating conditions of the reactor over that range. This single exposure step is then referred to as the "state point". Table 3-3 shows the number of state points used for each cycle in this fluence evaluation.

#### **3.4.3.2 Projected Reactor Operation**

Projections of plant operations beyond cycle 19 are represented by an "equilibrium" cycle that incorporates the best-available information on expected cycle length, fuel bundle loading, and operating strategies for future cycles beyond cycle 19. Based on evaluations of the most recently completed cycles, cycle 18 is used as the equilibrium cycle for this analysis to project fluence to the end of the extended plant design life of 56 EFPY. Cycle 19 experienced an atypical core power shape due to the insertion of peripheral control rods for more than two-thirds of the cycle. Since cycle 18 has a similar core loading and rated power level with a symmetric power shape, it will provide a more representative estimate of the operating conditions over the plant's life.

### 3.4.3.3 Limitation of Fluence Projections

The fluence values presented in this report are based on projections of HC1's operations beyond the current operating cycle. Projections are performed using an assumed equilibrium cycle. The significance of the equilibrium cycle is that it defines the flux profiles that are used to project fluence into the future. Providing that the design basis for the equilibrium cycle does not change appreciably, projections based on the equilibrium cycle should remain bounding through 56 EFPY to support licensing, in-service inspection, and flaw evaluation activities.

If the design basis for the equilibrium cycle changes at any point in time, thereby producing a significant change to the flux profiles for the equilibrium cycle, then a new evaluation is needed. Operating conditions, if changed, that could impact the validity of the equilibrium cycle include power uprates, introduction of new fuel designs, changes in projected cycle lengths, changes in core loading strategies, changes in reactor flow, or other changes that could alter the flux profiles used in the fluence projections.

A summary of the operational characteristics of the projection cycle, cycle 18, are presented in Table 3-4. Figure 3-2 illustrates the relative powers of the fuel assemblies used in the model for the projection cycle and Figure 3-3 shows the cycle average peripheral axial power profile. Both are based on the average assembly burnup from the first state point to the last and, therefore, don't incorporate the cycle startup and shutdown time periods.

**Table 3-4**  
**Projection Cycle Operating Characteristics**

Characteristic	Value
Dominant Fuel Design	GE14
Dominant Peripheral Fuel Design	GE14
Core Rated Power	3840 MWt
Cycle Length (approx.)	521 days
Effective Power Factor (approx.)	0.97

	16	17	18	19	20	21	22	23	24	25	26	27	28	29	30
1	0.446	0.449	0.444	0.432	0.402	0.369	0.321								
2	0.852	0.862	0.857	0.841	0.796	0.745	0.645	0.419							
3	0.902	1.143	1.065	1.014	0.854	0.946	0.739	0.702	0.420	0.260					
4	1.245	0.991	1.227	0.976	1.166	1.144	1.105	0.776	0.713	0.390					
5	1.042	1.285	1.197	1.284	1.183	1.250	1.012	1.111	0.775	0.573	0.370				
6	1.250	1.101	1.317	1.071	1.297	1.076	1.253	1.151	0.975	0.737	0.539	0.386	0.257		
7	0.952	1.289	1.214	1.052	1.148	1.293	1.198	1.096	0.901	0.975	0.772	0.710	0.418		
8	1.074	1.085	1.302	1.031	1.163	1.075	1.310	0.988	1.094	1.149	1.108	0.774	0.703	0.417	
9	1.108	1.363	1.137	1.306	1.074	1.328	1.236	1.310	1.198	1.252	1.011	1.103	0.738	0.645	0.322
10	1.347	1.122	1.315	1.217	1.343	1.130	1.327	1.074	1.293	1.076	1.248	1.143	0.946	0.746	0.371
11	1.015	1.289	1.037	1.073	0.951	1.344	1.074	1.163	1.148	1.297	1.182	1.166	0.854	0.799	0.418
12	1.126	1.199	1.258	0.934	1.073	1.217	1.305	1.030	1.051	1.071	1.284	0.977	1.014	0.841	0.434
13	1.022	1.287	1.034	1.257	1.037	1.317	1.137	1.301	1.213	1.318	1.196	1.227	1.064	0.858	0.445
14	1.227	1.223	1.288	1.198	1.288	1.122	1.362	1.083	1.287	1.101	1.283	0.991	1.142	0.862	0.449
15	0.867	1.227	1.021	1.125	1.013	1.347	1.107	1.073	0.949	1.250	1.042	1.242	0.903	0.853	0.446

**Figure 3-2  
Projection Cycle Relative Power Map (PANAC Fuel Coordinates)**

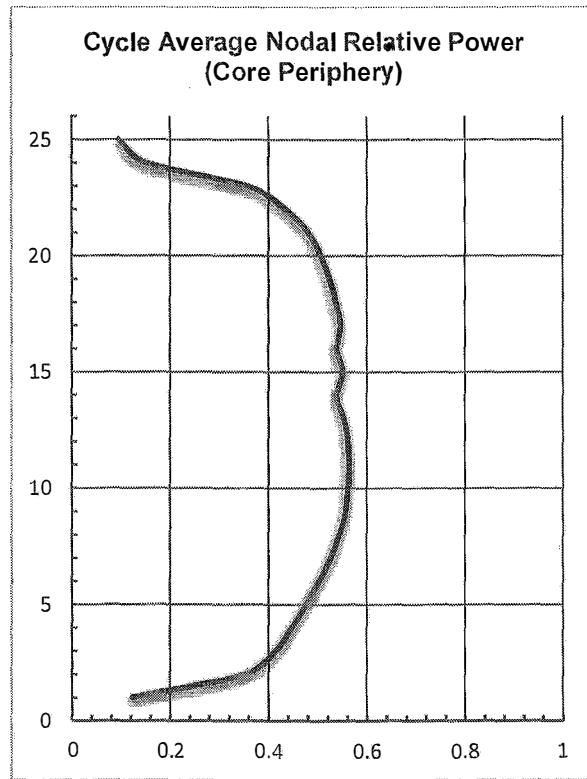


Figure 3-3  
Projection Cycle Average Nodal Relative Power Axial Profile (Core Periphery)

# 4

## CALCULATION METHODOLOGY

This section provides an overview of the HC1 fluence model that was developed with the RAMA Fluence Methodology software [1]. The RAMA fluence model for HC1 is a plant-specific model that was constructed from the design inputs described in Section 3, *Description of the Reactor System*.

### 4.1 Description of the RAMA Fluence Methodology

The RAMA Fluence Methodology (RAMA) is a system of computer codes, a data library, and an uncertainty methodology that determines best-estimate fluence in light water reactor pressure vessels and vessel components. The primary codes that comprise the RAMA methodology include model builder codes, a particle transport code, and a fluence calculator code. The data library contains nuclear cross sections and response functions that are needed for each of the codes. The uncertainty methodology is used to determine the uncertainty and bias in the best-estimate fluence calculated by the software.

The primary inputs for RAMA are mechanical design parameters and reactor operating history data. The mechanical design inputs are obtained from plant-specific design drawings, which include as-built measurements when available. The reactor operating history data is obtained from reactor core simulator codes, system heat balance calculations and daily operating logs that describe the operating conditions of the reactor over its operating lifetime. The primary outputs from RAMA calculations are neutron flux, neutron fluence, dosimetry activation, and an uncertainty evaluation.

The model builder codes consist of geometry and material processor codes that generate input for the particle transport code. The geometry model builder code uses mechanical design inputs and meshing specifications to generate three-dimensional geometry models of the reactor. The material processor code uses reactor operating data inputs to process fuel materials, structural materials, and water densities that are consistent with the geometry meshing generated by the geometry model builder code.

The particle transport code performs three-dimensional neutron flux calculations using a deterministic, multigroup, particle transport theory method with anisotropic scattering. The primary inputs prepared by the user for the transport code include the geometry and material data generated by the model builder codes and numerical integration and convergence parameters for the iterative transport calculation. The transport solver is coupled with a general geometry modeling capability based on combinatorial geometry techniques. The coupling of general geometry with a deterministic transport solver provides a flexible, accurate, and efficient tool for

calculating neutron flux in light water reactor pressure vessels and vessel components. The primary output from the transport code is the neutron flux in multigroup form.

The fluence calculator code determines fluence and activation in the reactor pressure vessel and vessel components over specified periods of reactor operation. The primary inputs to the fluence calculator include the multigroup neutron flux from the transport code, response functions for the various materials in the reactor, reactor power levels for the operating periods of interest, the specification of which components to evaluate, and the energy ranges of interest for evaluating neutron fluence. The fluence calculator includes treatments for isotopic production and decay that are required to calculate specific activities for irradiated materials. The reactor operating history is generally represented with several reactor state points that represent the various power levels and core power shapes generated by the reactor over the life of the plant. These detailed state points are combined with the daily reactor power levels to produce accurate estimates of the fluence and activations accumulated in the plant.

The uncertainty methodology provides an assessment of the overall accuracy of the RAMA Fluence Methodology. Variances in the dimensional data, reactor operating data, dosimetry measurement data, and nuclear data are evaluated to determine if there is a statistically significant bias in the calculated results that might affect the determination of the best-estimate fluence for the reactor. The plant-specific results are also weighted with comparative results from experimental benchmarks and other plant analyses and analytical uncertainties pertaining to the methodology to determine if the plant-specific model under evaluation is statistically acceptable as defined in Regulatory Guide 1.190.

The RAMA nuclear data library contains atomic mass data, nuclear cross-section data, and response functions that are needed in the material processing, transport, fluence, and reaction rate calculations. The cross-section data and response functions are based on the BUGLE-96 nuclear data library [22] and the VITAMIN-B6 data library [23].

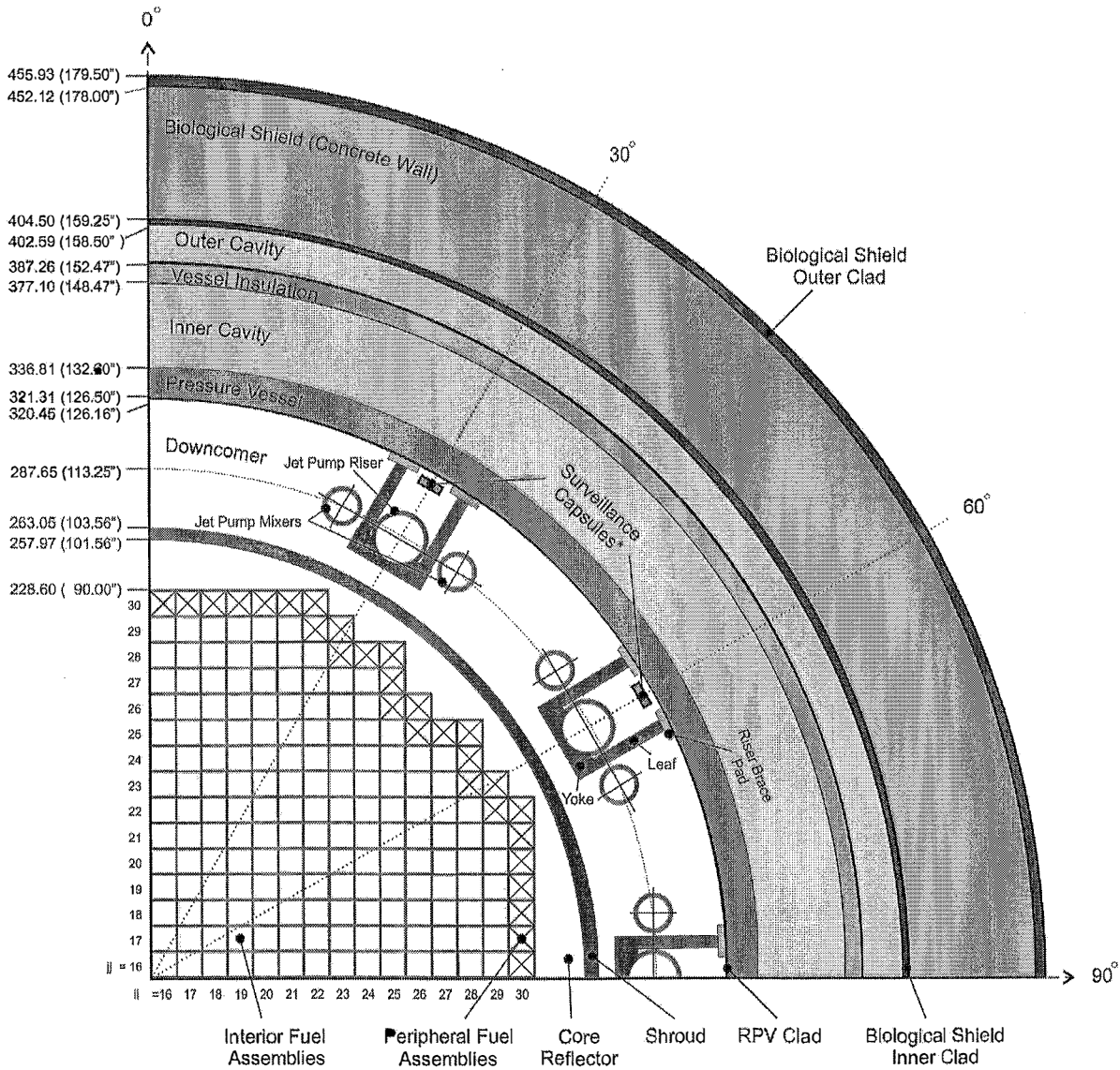
## 4.2 The RAMA Geometry Model for the HC1 Reactor

Section 3, *Description of the Reactor System*, describes the design inputs that were provided by PSEG for the HC1 reactor fluence evaluation. These design inputs were used to develop a plant specific, three-dimensional computer model of the HC1 reactor with the RAMA Fluence Methodology.

Figure 4-1 and Figure 4-2 provide general illustrations of the primary components, structures and regions developed for the HC1 fluence model. Figure 4-1 shows the planar configuration of the reactor model at an elevation corresponding to the reactor core mid-plane elevation. Figure 4-2 shows an axial configuration of the reactor model. Note that the figures are not drawn to scale. They are intended only to provide a perspective for the layout of the model, and specifically how

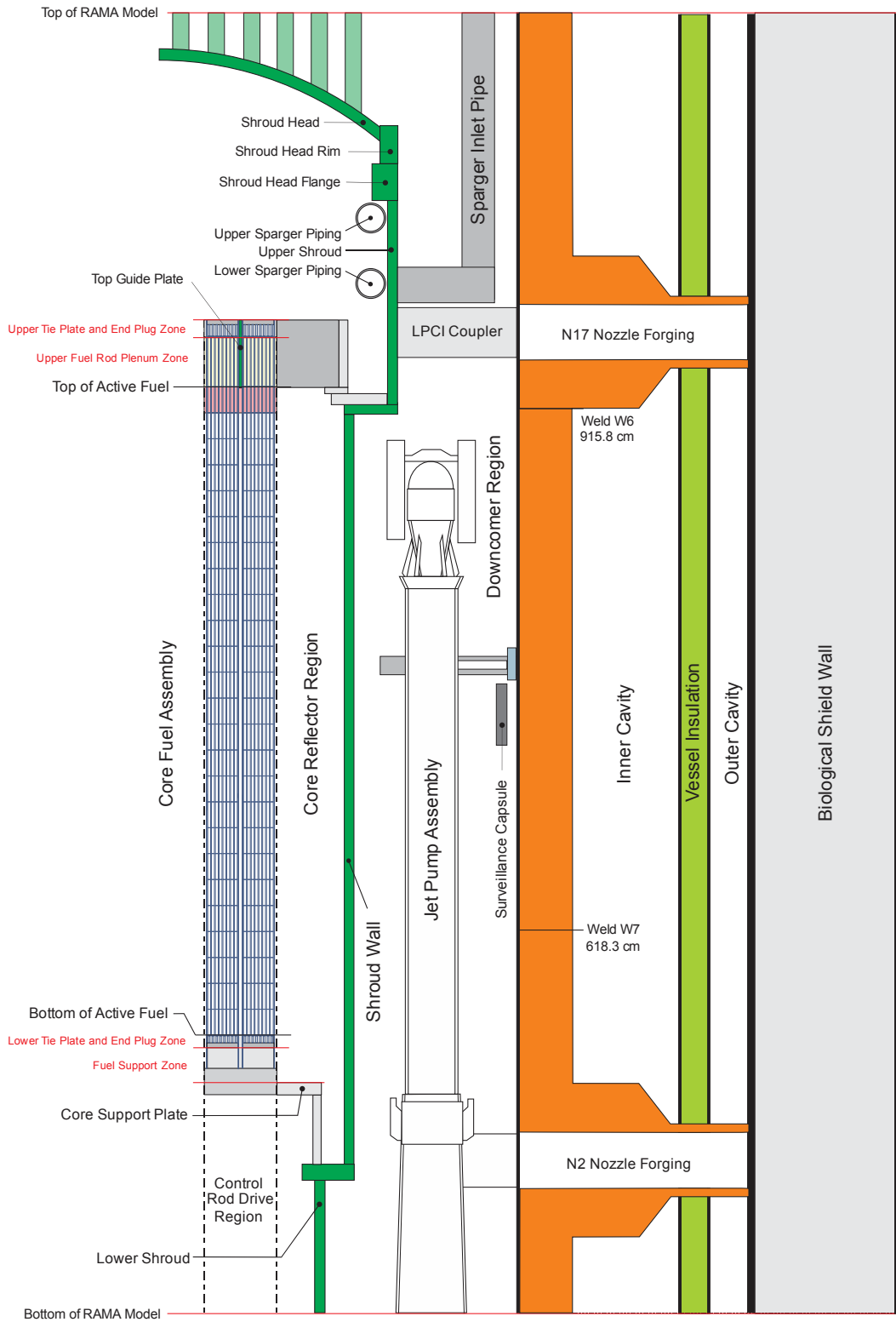
the various components, structures, and regions lie relative to the reactor core region (i.e., the neutron source).

Because the figures are intended only to provide a general overview of the model, they do not include illustrations of the geometry meshing developed for the model. To provide such detail is beyond the scope of this document.



Notes: This drawing is not to scale.  
 Dimensions are given in centimeters (inches), rounded to two decimal places.  
 \* In quadrant symmetry, these capsules represent the 30°, 120° and 300° capsules

**Figure 4-1**  
**Planar View of the HC1 RAMA Quadrant Model at the Core Mid-Plane Elevation**



Notes: This drawing is not to scale.

**Figure 4-2**  
**Axial View of the HC1 RAMA Model**

The following subsections provide an overview of the computer models that were developed for the various components, structures, and coolant flow regions of the HC1 reactor.

#### **4.2.1 The Geometry Model**

RAMA uses a generalized three-dimensional geometry modeling system that is based on a combinatorial geometry technique, which is mapped to a Cartesian coordinate system. In this analysis, an axial plane of the reactor model is defined by the (x,y) coordinates of the modeling system and the axial elevation at which a plane exists is defined along a perpendicular z-axis of the modeling system. Thus, any point in the reactor model can be addressed by specifying the (x,y,z) coordinates for that point.

Figure 3-1 of Section 3 illustrates a planar cross-section view of the HC1 reactor design at an axial elevation corresponding to the reactor core mid-plane elevation. It is shown for this one elevation that the reactor design is a complex geometry composed of various combinations of rectangular, cylindrical, and wedge-shaped bodies. When the reactor is viewed in three dimensions, the varying heights of the different components, structures, and regions create additional geometry modeling complexities. An accurate representation of these geometrical complexities in a predictive computer model is essential for calculating accurate, best-estimate fluence in the reactor pressure vessel, the vessel internals, and the surrounding structures.

Figure 4-1 and Figure 4-2 provide general illustrations of the planar and axial geometry complexities that are represented in the HC1 fluence model. For comparison purposes, the planar view illustrated in Figure 4-1 corresponds to the same core mid-plane elevation illustrated in Figure 3-1. The computer model for HC1 assumes azimuthal quadrant symmetry in the planar dimension.

Figure 4-1 illustrates the quadrant geometry that was modeled in this analysis. In terms of the modeling coordinate system, the “northeast” quadrant of the geometry is represented in the model. The 0-degree azimuth, which has a “north” designation, corresponds to the 0-degree azimuth referenced in the plant drawings for the reactor pressure vessel. Degrees are incremented clockwise. Thus, the 90-degree azimuth is designated as the “east” direction. All other components, structures, and regions have been appropriately mirror reflected or rotated to this quadrant based upon their relationship to the pressure vessel orientation to ensure that the fluence is appropriately calculated relative to the neutron source (i.e., the core region). Although symmetry is a modeling consideration, the results presented in this report for the different components and structures are given at their correct azimuths in the plant.

Figure 4-2 illustrates the axial configuration of the primary components, structures, and regions in the fluence model. For discussion purposes, the same components, structures, and regions shown in the planar view of Figure 4-1 are also illustrated in Figure 4-2. Figure 4-2 shows that the axial height of the fluence model spans from a lower elevation just below the N2 nozzle forging to above

the core shroud head. This axial height covers all areas of the reactor pressure vessel that are expected to exceed a fluence threshold of  $1.0E+17$  n/cm<sup>2</sup> at 56 EFPY.

As previously noted, Figure 4-1 and Figure 4-2 are not drawn precisely to scale. They are intended only to provide a perspective of how the various components, structures, and regions of the reactor are positioned relative to the reactor core region (i.e., the neutron source) and each other. The following subsections provide details on the modeling of individual components, structures, and regions. Please refer to the figures for visual orientation of the components and regions described in the following subsections.

#### **4.2.2 The Reactor Core and Core Reflector Models**

The reactor core contains the nuclear fuel that is the source of the neutrons that irradiate all components and structures of the reactor. The core is surrounded by a shroud structure that serves to channel the reactor coolant through the core region during reactor operation. The region between the core and the core shroud is the core reflector, and it contains coolant. The reactor core geometry is rectangular in design and is modeled with rectangular elements to preserve its shape in the analysis. The core reflector region interfaces with the rectangular shape of the core region and the curved shape of the core shroud. It is, therefore, modeled using a combination of rectangular and cylindrical elements.

The core region is centered in the reactor pressure vessel and is characterized in the analysis with two fundamental fuel zones: interior fuel assemblies and peripheral fuel assemblies. The peripheral fuel assemblies are the primary contributors to the neutron source in the fluence calculation. Because these assemblies are loaded at the core edge where neutron leakage from the core is greatest, there is a sharp power gradient across these assemblies that requires consideration. To account for the power gradient, the peripheral fuel assemblies are sub-meshed with additional elements that preserve the pin-wise details of the fuel assembly geometry and power distribution. The interior fuel assemblies make a lesser contribution to the reactor fluence and are, therefore, modeled in various homogenized forms in accordance with their contributions to the reactor fluence. For computational efficiency, homogenization treatments are used in the interior core region primarily to reduce the number of mesh regions that must be solved in the transport calculation. The meshing configuration for each fuel assembly location in the core region is determined by parametric studies to ensure an accurate estimate of fluence throughout all regions of the reactor system.

Each fuel assembly design, whether loaded in the interior or peripheral locations in the core, is represented with four axial material zones: the lower tie plate/end plug zone, the fuel zone, the fuel upper plenum zone, and the upper tie plate/end plug zone. The structural materials in the top and bottom nozzles for each unique assembly design are represented in the model to address the shielding effects that these materials have on the components above and below the core region. The fuel zone contains the nuclear fuel and structural materials for the fuel assemblies. The

materials for each fuel assembly are unique during reactor operation and are incorporated into the model using reactor operating data from core simulator codes. The upper plenum region captures fission gases during reactor operation.

The HC1 reactor core region has a nominal elevation for the bottom of active fuel at 549.4274 cm (216.31") and an active fuel height of 381.00 cm (150"). The core simulator codes used by HC1 modeled the core as 150" in all situations, so this value was also used in the RAMA model. From an isotopic standpoint, the core is modeled using quadrant symmetry. For the vessel internal component fluence evaluations, the NE fuel quadrant was used.

#### **4.2.3 The Core Shroud Model**

The core shroud is a canister-like structure that contains the reactor core and channels the reactor coolant and steam produced by the core into the steam separators. Axially the shroud extends almost the entire height of the model, from the lower shroud wall to the top of the shroud head rim. There are several circumferential and vertical welds on the shroud. The core shroud is cylindrical in design and is modeled with pipe elements.

The model also includes an accurate representation of the shroud head. It is modeled with spherical elements and includes the penetrations and piping for the steam separator stand pipes. The stand pipes are modeled with pipe elements.

#### **4.2.4 The Downcomer Region Model**

The downcomer region lies between the core shroud and the reactor pressure vessel. It is basically cylindrical in design, but with some geometrical complexities created by the presence of jet pumps and surveillance capsules in the region. The majority of the downcomer region is modeled with pipe segments. The areas of the downcomer containing the jet pumps and specimen capsules are modeled with the appropriate geometry elements to represent their design features and to preserve their radial, azimuthal, and axial placement in the downcomer region. These structures are described further in the following subsections.

#### **4.2.5 The Jet Pump Model**

There are ten jet pump assemblies in the downcomer region of HC1, which provide the main recirculation flow for the core. The jet pumps are modeled at azimuths 30, 60, and 90 degrees in the downcomer region. When symmetry is applied to the model, the 30-degree location represents the jet pump assemblies that are positioned azimuthally at 30, 150, 210, and 330 degrees; the 60-degree location represents those at 60, 120, 240, and 300 degrees; and the 90-degree location represents the jet pump assemblies at 90 and 270 degrees.

The jet pump model includes representations for the riser, mixer, and diffuser pipes; nozzles; rams head; hold-down beams and brackets; riser inlet pipe; and riser brace yoke, leafs, and pads. The jet pump assembly design is modeled using cylindrical pipe elements for the jet pump riser and mixer pipes. The riser pipe is correctly situated between the centers of the mixer pipes. Cylinders intersected with wedges are used to represent the rams head. The riser brace assembly model includes two leaf structures that attach to the yoke and pad elements. The jet pump assembly includes hold down beams and brackets, built with rectangular boxes, which are attached to the rams head.

The jet pump repair hardware, including the auxiliary spring wedges and slip-joint clamps, are not explicitly included in the model. Evaluations of the repair hardware components are performed using the flux from the downcomer regions where the components would exist. Since the surface fluence represents the peak based on their orientation to the core, this approach has a negligible effect on the results.

#### **4.2.6 The Surveillance Capsule Model**

The surveillance capsules are installed near the inner surface of the pressure vessel wall. The surveillance capsules are rectangular in design. Because of this shape, the capsules are not easily implemented in the otherwise cylindrical elements of the downcomer region model. With reference to Figure 3-1, it is observed that the capsules are of small dimensions in the planar geometry and they reside a long distance (view factor) from the core region. Based on these factors, the otherwise rectangular shape of the surveillance capsules can be reasonably approximated in the model with arc elements. The surveillance capsule model also includes a representation for the downcomer water that surrounds the capsule on all sides.

The surveillance capsules are correctly modeled behind the jet pump riser pipes at the 30- and 60-degree azimuths based on the as-built dimensions of the lower capsule mounting bracket. When symmetry is applied to the model, the 30-degree location represents the capsule installed at 30 degrees, while the 60-degree location represents the capsules at 120 and 300 degrees.

The surveillance capsules are modeled at their correct axial position and height relative to the core region. The surveillance capsules cover about nine percent of the total core height.

#### **4.2.7 The Reactor Pressure Vessel Model**

The reactor pressure vessel and vessel cladding lie outside the downcomer region and each is cylindrical in design. Both are modeled with pipe elements. The cladding-pressure vessel interface is a key location for RPV fluence calculations and is preserved in the model. This interface defines the inside surface (OT) for the pressure vessel base metal where the RPV fluence is calculated. HC1 has cladding only on the inside surface of the pressure vessel wall. Representations of the

forgings for the recirculation inlet (N2) and LPCI (N17) nozzles are also included in the model out to the biological shield radius. The nozzle representations are modeled in their true conical shape.

#### **4.2.8 The Vessel Insulation Model**

The vessel insulation lies in the cavity region outside the pressure vessel wall. The insulation is cylindrical in design and follows the contour of the pressure vessel wall. It is modeled with pipe elements.

#### **4.2.9 The Inner and Outer Cavity Models**

The cavity region lies between the pressure vessel and biological structures. As previously described, the vessel insulation lies in the cavity region; thus creating two cavity regions. The inner cavity region lies between the vessel and the insulation. The outer cavity region lies between the vessel insulation and biological shield cladding. The boundaries of the cavity regions follow the contours of the pressure vessel, vessel insulation, and biological shield. The cavity regions are essentially cylindrical in design and are modeled with pipe segments.

#### **4.2.10 The Biological Shield Model**

The biological shield (concrete) defines the outer most region of the fluence model. The biological shield is basically cylindrical in design and is modeled with pipe segments. There is cladding on the inside and outside surface of the biological shield.

#### **4.2.11 The Above-Core Component Models**

Figure 4-2 includes illustrations of other components and regions that lie above the reactor core region. The predominant above-core components represented in the model include the top guide and core spray spargers.

##### **4.2.11.1 The Top Guide Model**

The top guide component lies above the core region. The top guide is appropriately modeled by including representations for the vertical fuel assembly parts and top guide plates. The upper fuel assembly parts that extend into the top guide region are modeled in three axial segments: the fuel rod plenum, fuel rod upper end plugs, and fuel assembly upper tie plate. The fuel assembly parts and top guide plates are modeled with rectangular elements.

##### **4.2.11.2 The Core Spray Sparger Model**

The core spray spargers include upper and lower sparger annulus pipes and inlet piping. The core spray sparger annulus pipes are appropriately represented as torus structures in the model. The sparger annulus pipes reside inside the upper shroud wall above the top guide. The spargers are

modeled as pipe-like structures and include a representation of reactor coolant inside the pipes. The model includes an accurate representation of the horizontal pipe extending from the penetration in the shroud, and the vertical pipe extending upwards to the top of the model.

#### **4.2.12 The Below-Core Component Models**

Figure 4-2 includes illustrations of other components and regions that lie below the reactor core region. The fuel support piece, core support plate, and core inlet regions appropriately include a representation of the cruciform control rod below the core region. The lower fuel assembly parts include representations for the fuel rod lower end plugs, lower tie plate, and nose piece. The below-core components are modeled with rectangular elements with the exception of the core support plate. The core support plate is modeled using both rectangular and cylindrical elements to provide an appropriate representation of that component. Core support plate rim bolts are included.

#### **4.2.13 Summary of the Geometry Modeling Approach**

To summarize the reactor modeling process, there are several key features of the RAMA code system that allow the reactor design to be accurately represented for RPV and component fluence evaluations. Following is a summary of some of the key features of the model.

- Rectangular, cylindrical, spherical, and wedge bodies are mixed in the model in order to provide an accurate geometrical representation of the components and regions in the reactor.
- The reactor core geometry is modeled with rectangular bodies to represent its actual shape in the reactor. The fuel assemblies in the core region are also sub-meshed with additional rectangular bodies to represent the pin cell regions in the assemblies.
- A combination of rectangular and cylindrical bodies is used to describe the transition parts between the rectangular core region and the cylindrical outer core regions.
- Cylindrical and wedge bodies are used to model the components and regions that extend outward from the core region (core shroud, downcomer, RPV, etc.).
- The surveillance capsules are modeled at their as-built radial, azimuthal, and elevational positions behind the jet pumps in the downcomer region.
- The above-core region includes accurate representations of the top guide and core spray spargers.
- The below-core region includes appropriate representations for the fuel support piece, core support plate and rim bolts, core inlet regions, cruciform control rods, and control rod guide tubes.
- The biological shield is appropriately represented as a cylindrical body, with cladding on the inside and outside surfaces.

### 4.3 RAMA Calculation Parameters

The RAMA transport code uses a three-dimensional deterministic transport method to calculate the neutron flux. The accuracy of the transport method is based on a numerical integration technique that uses ray-tracing to characterize the geometry, anisotropy treatments to determine the directional flow of particles, and convergence parameters to determine the overall accuracy of the flux solution between iterations. The code allows the user to specify values for each of these parameters.

The primary input parameters that control the ray-tracing calculation are the distance between parallel rays in the planar and axial dimensions, the depth that a particle is tracked when a reflective boundary is encountered, and the number of equally spaced angles in polar coordinates for tracking the particles. Plant-specific values are determined for each of the parameters. The RAMA transport calculation employs a treatment for anisotropy that is based on a Legendre expansion of the scattering cross sections. By default, the RAMA transport calculation uses the maximum order of expansion that is available for each nuclide in the RAMA nuclear data library. For the actinide and zirconium nuclides, a P<sub>5</sub> expansion of the scattering cross sections is used. For all other nuclides, a P<sub>7</sub> expansion of the scattering cross sections is used.

The overall accuracy of the neutron flux calculation is determined using an iterative technique to converge the flux iterations. The convergence criterion used in the evaluation was determined by parametric study to provide an asymptotic solution for this model.

### 4.4 RAMA Neutron Source Calculation

RAMA calculates a unique neutron source distribution for each transport calculation using the input relative power density factors for the fuel region and data from the RAMA nuclear data library. The source distribution changes with fuel burnup; thus, the source is determined using core-specific three-dimensional burnup distributions at frequent intervals throughout a cycle. For the fluence model, the peripheral fuel assemblies are modeled to preserve the power gradient at the core edge that is formed from the pin-wise source distributions in these fuel assemblies.

### 4.5 RAMA Fission Spectra

RAMA calculates a weighted fission spectrum for each transport calculation that is based on the relative contributions of <sup>235</sup>U, <sup>238</sup>U, <sup>239</sup>Pu, <sup>240</sup>Pu, <sup>241</sup>Pu, and <sup>242</sup>Pu isotopes. The fission spectra for these isotopes are derived from the BUGLE-96 nuclear data library.

# 5

## SURVEILLANCE CAPSULE ACTIVATION AND FLUENCE RESULTS

This section documents the activation results for HC1. The activation results form the basis for the validation and qualification of the application of the RAMA Fluence Methodology to HC1 in accordance with the requirements of U. S. NRC Regulatory Guide 1.190 (Reg. Guide 1.190). Reg. Guide 1.190 requires fluence calculational methods to be validated by comparison with measurements from operating reactor dosimetry for the specific plant being analyzed or for reactors of similar design. The acceptance criteria provided in Reg. Guide 1.190 is that the comparison to measurement ratios (C/M) and standard deviation values must be  $\leq 20\%$ . All of the HC1 reactor capsule measurements comparisons to the RAMA predicted values meet the Reg. Guide 1.190 limits. The accuracy of the comparisons is additional confirmation that the RAMA Fluence Methodology provides unbiased fluence estimates for the HC1 reactor dosimetry.

Three flux wire activation analyses were performed for HC1. Flux wires were removed from the 30-degree capsule flux wire holder and analyzed at the end of cycle 1 (irradiated for 1.0 EFPY); surveillance capsule flux wires were removed at the end of cycle 5 from the 30-degree capsule (irradiated for 6.0 EFPY); and surveillance capsule flux wires were removed at the end of cycle 19 from the 120-degree capsule (irradiated for 24.1 EFPY). Details of the dosimetry specimens and analysis are presented in Section 5.1.

During the evaluation process, it was observed that the calculated activity overestimated the capsule measurements by 10-20% for both the cycle 5 and cycle 19 capsule pulls. While this conservatism was originally observed in a previous evaluation [20], it was reasoned at that time as possibly being linked to the coarseness of the nodal data used in modeling the early cycles of operation. However, cycle 19 is based on a detailed pin-by-pin power representation, along with all other cycles beyond cycle 5. Observing the same or greater conservatism in the cycle 19 capsule indicates a different source for the over-estimation.

Upon reviewing the previous evaluation and plant drawings, it was further noted that the as-built surveillance capsule mounting bracket bail-to-RPV-clad distance was well outside of the nominal dimensions. Plant drawings indicate that the bail is nominally located about 3.0 cm (1.18") from the cladding inner surface. As-built drawings indicate this distance to be between 3.75 and 3.80 cm (1.48-1.50"). While no direct tolerance for the dimension is identified, the standard tolerance for decimal dimensions is given as  $\pm 0.15$  cm ( $\pm 0.06$  in), indicating that the bracket is out of specification.

The difference between the nominal and as-built dimensions also appears to very closely match the nominal RPV cladding thickness of 0.85 cm (0.33 in), indicating that perhaps the discrepancy

in the as-built dimensions is that they are reported relative to the RPV base metal instead of to the cladding inner surface. Since no resolution can be definitively reached at this time, results are provided for all capsules at both the nominal and as-built locations. Note that the bracket dimensioning has a negligible effect on the EOC 1 flux wire holder since the holder is attached to an arm which is bent to be in contact with the RPV clad inner surface, making its position relatively insensitive to changes in the capsule radial location. Given the good agreement between calculation and measurements for the flux wire holder, it can be assumed that the RPV wall inner radius is not the source of the error with the capsule evaluations.

## **5.1 Comparison of Predicted Activation to Plant-Specific Measurements**

The comparison of predicted activation for the HC1 cycles 1, 5, and 19 flux wires to measurements is presented in this subsection. Note that the precise location of the individual wires within the surveillance capsule flux wire holder and surveillance capsule holders is not known, therefore, the activation calculations were performed at the center of the respective holders.

### **5.1.1 Cycle 1 30-Degree Flux Wire Holder Activation Analysis**

Copper and iron flux wires were removed from the flux wire holder attached to the 30-degree surveillance capsule container at the end of cycle 1. These flux wires were irradiated for a total of 1.0 EFPY. Activation measurements were performed for the flux wires for the following reactions [24]:  $^{63}\text{Cu}(n,\alpha)^{60}\text{Co}$  and  $^{54}\text{Fe}(n,p)^{54}\text{Mn}$ .

Table 5-1 provides a comparison of the RAMA calculated-to-measured (C/M) specific activities for the flux wire specimens. The total average C/M results for all flux wires is 1.01 with a standard deviation of  $\pm 0.06$ . The average C/M for the copper flux wires is 0.95 with a standard deviation of  $\pm 0.01$ . The average C/M for the iron flux wires is 1.06 with a standard deviation of  $\pm 0.01$ . The C/M results show acceptable agreement between the RAMA calculated values and the measured values.

The fast neutron fluence for the HC1 cycle 1 flux wires was determined by RAMA to be  $2.42\text{E}+16$  n/cm<sup>2</sup> for energy >1.0 MeV at 1.0 EFPY.

**Table 5-1  
Comparison of Specific Activities for the HC1 Cycle 1 Flux Wire Holder Wires (C/M)**

Flux Wires	Measured (dps/g)	Calculated (dps/g)	Calculated vs. Measured	Standard Deviation
<b>Copper</b>				
Cu-1	1.85E+03	1.78E+03	0.96	
Cu-2	1.87E+03	1.78E+03	0.95	
Cu-3	1.86E+03	1.78E+03	0.95	
<b>Average</b>	<b>1.86E+03</b>	<b>1.78E+03</b>	<b>0.95</b>	<b>0.01</b>
<b>Iron</b>				
Fe-1	4.20E+04	4.45E+04	1.06	
Fe-2	4.24E+04	4.45E+04	1.05	
Fe-3	4.20E+04	4.45E+04	1.06	
<b>Average</b>	<b>4.21E+04</b>	<b>4.45E+04</b>	<b>1.06</b>	<b>0.01</b>
<b>Total Flux Wire Average</b>	---	---	<b>1.01</b>	<b>0.06</b>

**5.1.2 Cycle 5 30-Degree Surveillance Capsule Activation Analysis**

Copper, iron, and nickel flux wires were irradiated in the HC1 surveillance capsule at the 30-degree azimuth during the first five cycles of operation. These wires were removed after being irradiated for a total of 6.0 EFPY. Activation measurements were performed for the flux wires for the following reactions [25]:  $^{63}\text{Cu}(n,\alpha)^{60}\text{Co}$ ,  $^{54}\text{Fe}(n,p)^{54}\text{Mn}$ , and  $^{58}\text{Ni}(n,p)^{58}\text{Co}$ .

Table 5-2 provides comparisons of the RAMA calculated specific activities and the measured specific activities for the flux wire specimens in terms of a calculated-to-measured (C/M) ratio using the as-built capsule dimensions. The cycle 5 capsule total flux wire average C/M ratio with as-built dimensions is 1.09 with a standard deviation of  $\pm 0.07$ . The average C/M ratio for the copper flux wires is 1.00 with a standard deviation of  $\pm 0.02$ , for the iron flux wires is 1.13 with a standard deviation of  $\pm 0.01$  and for the nickel flux wires is 1.15 with a standard deviation of  $\pm 0.02$ . The C/M comparisons show acceptable agreement between the RAMA calculated values and the measured values.

Table 5-3 provides comparisons of the RAMA calculated specific activities and the measured specific activities for the flux wire specimens in terms of a calculated-to-measured (C/M) ratio using the nominal capsule dimensions. The cycle 5 capsule total flux wire average C/M ratio with

nominal dimensions is 0.97 with a standard deviation of  $\pm 0.06$ . The average C/M ratio for the copper flux wires is 0.89 with a standard deviation of  $\pm 0.02$ , for the iron flux wires is 1.00 with a standard deviation of  $\pm 0.01$  and for the nickel flux wires is 1.03 with a standard deviation of  $\pm 0.02$ . The C/M comparisons show acceptable agreement between the RAMA calculated values and the measured values.

The fast neutron fluence for the HC1 cycle 5 surveillance capsule flux wires was determined by RAMA to be  $1.81E+17$  n/cm<sup>2</sup> using as-built dimensions, and  $1.64E+17$  n/cm<sup>2</sup> using nominal dimensions, for energy >1.0 MeV at 6.0 EFPY.

**Table 5-2  
Comparison of Specific Activities for HC1 Cycle 5 Surveillance Capsule Flux Wires Using As-Built Dimensions (C/M)**

Flux Wires	Measured (dps/g)	Calculated (dps/g)	Calculated vs. Measured	Standard Deviation
<b>Copper</b>				
Copper 1	9.47E+03	9.30E+03	0.98	
Copper 2	9.31E+03	9.30E+03	1.00	
Copper 3	9.15E+03	9.30E+03	1.02	
<b>Average</b>	<b>9.31E+03</b>	<b>9.30E+03</b>	<b>1.00</b>	<b>0.02</b>
<b>Iron</b>				
Iron 1	8.92E+04	1.01E+05	1.14	
Iron 2	9.08E+04	1.01E+05	1.12	
Iron 3	9.02E+04	1.01E+05	1.13	
<b>Average</b>	<b>9.01E+04</b>	<b>1.01E+05</b>	<b>1.13</b>	<b>0.01</b>
<b>Nickel</b>				
Nickel 1	1.31E+06	1.52E+06	1.16	
Nickel 2	1.34E+06	1.52E+06	1.13	
Nickel 3	1.31E+06	1.52E+06	1.16	
<b>Average</b>	<b>1.32E+06</b>	<b>1.52E+06</b>	<b>1.15</b>	<b>0.02</b>
<b>Total Flux Wire Average</b>	---	---	<b>1.09</b>	<b>0.07</b>

**Table 5-3  
Comparison of Specific Activities for HC1 Cycle 5 Surveillance Capsule Flux Wires Using Nominal Dimensions (C/M)**

Flux Wires	Measured (dps/g)	Calculated (dps/g)	Calculated vs. Measured	Standard Deviation
<b>Copper</b>				
Copper 1	9.47E+03	8.30E+03	0.88	
Copper 2	9.31E+03	8.30E+03	0.89	
Copper 3	9.15E+03	8.30E+03	0.91	
<b>Average</b>	<b>9.31E+03</b>	<b>8.30E+03</b>	<b>0.89</b>	<b>0.02</b>
<b>Iron</b>				
Iron 1	8.92E+04	9.01E+04	1.01	
Iron 2	9.08E+04	9.01E+04	0.99	
Iron 3	9.02E+04	9.01E+04	1.00	
<b>Average</b>	<b>9.01E+04</b>	<b>9.01E+04</b>	<b>1.00</b>	<b>0.01</b>
<b>Nickel</b>				
Nickel 1	1.31E+06	1.35E+06	1.03	
Nickel 2	1.34E+06	1.35E+06	1.01	
Nickel 3	1.31E+06	1.35E+06	1.03	
<b>Average</b>	<b>1.32E+06</b>	<b>1.35E+06</b>	<b>1.03</b>	<b>0.02</b>
<b>Total Flux Wire Average</b>	---	---	<b>0.97</b>	<b>0.06</b>

### 5.1.3 Cycle 19 120-Degree Surveillance Capsule Activation Analysis

Copper, iron, and nickel flux wires were irradiated in the HC1 surveillance capsule at the 120-degree azimuth during the first nineteen cycles of operation. These wires were removed after being irradiated for a total of 24.1 EFPY. Activation measurements were performed for the flux wires for the following reactions [26]:  $^{63}\text{Cu}(n,\alpha)^{60}\text{Co}$ ,  $^{54}\text{Fe}(n,p)^{54}\text{Mn}$ , and  $^{58}\text{Ni}(n,p)^{58}\text{Co}$ .

Table 5-4 provides comparisons of the RAMA calculated specific activities and the measured specific activities for the flux wire specimens in terms of a calculated-to-measured (C/M) ratio using the as-built dimensions. The cycle 19 capsule total flux wire average C/M ratio with as-built dimensions is 1.16 with a standard deviation of  $\pm 0.06$ . The average C/M ratio for the copper flux

wires is 1.09 with a standard deviation of  $\pm 0.02$ , for the iron flux wires is 1.18 with a standard deviation of  $\pm 0.00$  and for the nickel flux wires is 1.21 with a standard deviation of  $\pm 0.01$ . The C/M comparisons show acceptable agreement between the RAMA calculated values and the measured values.

Table 5-5 provides comparisons of the RAMA calculated specific activities and the measured specific activities for the flux wire specimens in terms of a calculated-to-measured (C/M) ratio using the nominal dimensions. The cycle 19 capsule total flux wire average C/M ratio with nominal dimensions is 1.03 with a standard deviation of  $\pm 0.05$ . The average C/M ratio for the copper flux wires is 0.97 with a standard deviation of  $\pm 0.02$ , for the iron flux wires is 1.05 with a standard deviation of  $\pm 0.00$  and for the nickel flux wires is 1.07 with a standard deviation of  $\pm 0.01$ . The C/M comparisons show acceptable agreement between the RAMA calculated values and the measured values.

The fast neutron fluence for the HC1 cycle 19 surveillance capsule flux wires was determined by RAMA to be  $6.94E+17$  n/cm<sup>2</sup> using as-built dimensions, and  $6.27E+17$  n/cm<sup>2</sup> using nominal dimensions, for energy  $>1.0$  MeV at 24.1 EFPY.

**Table 5-4  
Comparison of Specific Activities for HC1 Cycle 19 Surveillance Capsule Flux Wires Using As-Built Dimensions (C/M)**

Flux Wires	Measured (dps/mg)	Calculated (dps/mg)	Calculated vs. Measured	Standard Deviation
<b>Copper</b>				
G8 Cu	1.52E+01	1.63E+01	1.07	
G9 Cu	1.49E+01	1.63E+01	1.09	
G10 Cu	1.48E+01	1.63E+01	1.10	
<b>Average</b>	<b>1.50E+01</b>	<b>1.63E+01</b>	<b>1.09</b>	<b>0.02</b>
<b>Iron</b>				
G8 Fe	9.67E+01	1.14E+02	1.18	
G9 Fe	9.69E+01	1.14E+02	1.18	
G10 Fe	9.61E+01	1.14E+02	1.18	
<b>Average</b>	<b>9.66E+01</b>	<b>1.14E+02</b>	<b>1.18</b>	<b>0.00</b>
<b>Nickel</b>				
G8 Ni	1.40E+03	1.68E+03	1.20	
G9 Ni	1.40E+03	1.68E+03	1.20	
G10 Ni	1.38E+03	1.68E+03	1.22	
<b>Average</b>	<b>1.39E+03</b>	<b>1.68E+03</b>	<b>1.21</b>	<b>0.01</b>
<b>Total Flux Wire Average</b>	---	---	<b>1.16</b>	<b>0.06</b>

**Table 5-5  
Comparison of Specific Activities for HC1 Cycle 19 Surveillance Capsule Flux Wires Using Nominal Dimensions (C/M)**

Flux Wires	Measured (dps/mg)	Calculated (dps/mg)	Calculated vs. Measured	Standard Deviation
<b>Copper</b>				
G8 Cu	1.52E+01	1.45E+01	0.95	
G9 Cu	1.49E+01	1.45E+01	0.97	
G10 Cu	1.48E+01	1.45E+01	0.98	
<b>Average</b>	<b>1.50E+01</b>	<b>1.45E+01</b>	<b>0.97</b>	<b>0.02</b>
<b>Iron</b>				
G8 Fe	9.67E+01	1.01E+02	1.05	
G9 Fe	9.69E+01	1.01E+02	1.04	
G10 Fe	9.61E+01	1.01E+02	1.05	
<b>Average</b>	<b>9.66E+01</b>	<b>1.01E+02</b>	<b>1.05</b>	<b>0.00</b>
<b>Nickel</b>				
G8 Ni	1.40E+03	1.49E+03	1.07	
G9 Ni	1.40E+03	1.49E+03	1.07	
G10 Ni	1.38E+03	1.49E+03	1.09	
<b>Average</b>	<b>1.39E+03</b>	<b>1.49E+03</b>	<b>1.07</b>	<b>0.01</b>
<b>Total Flux Wire Average</b>	---	---	<b>1.03</b>	<b>0.05</b>

**5.1.4 Surveillance Capsule Activation Analysis Summary**

Table 5-6 presents a summary of the total average calculated-to-measured result of specific activities for all HC1 flux wires using as-built dimensions. Combining all flux wires (copper, iron and nickel), the total average C/M is 1.10 with a standard deviation of ±0.09.

Table 5-7 presents a summary of the total average calculated-to-measured result of specific activities for all HC1 flux wires using nominal dimensions. Combining all flux wires (copper, iron and nickel), the total average C/M is 1.00 with a standard deviation of ±0.06.

**Table 5-6  
Comparison of Activities for HC1 Flux Wires Using As-Built Dimensions**

<b>Dosimeter</b>	<b>Number of Measurements</b>	<b>Calculated vs. Measured</b>	<b>Standard Deviation</b>
30-Degree Flux Wire (EOC 1)	6	1.01	0.06
30-Degree Capsule (EOC 5)	9	1.09	0.07
120-Degree Capsule (EOC 19)	9	1.16	0.06
<b>Total Flux Wire Average</b>	<b>24</b>	<b>1.10</b>	<b>0.09</b>

**Table 5-7  
Comparison of Activities for HC1 Flux Wires Using Nominal Dimensions**

<b>Dosimeter</b>	<b>Number of Measurements</b>	<b>Calculated vs. Measured</b>	<b>Standard Deviation</b>
30-Degree Flux Wire (EOC 1)	6	1.01	0.06
30-Degree Capsule (EOC 5)	9	0.97	0.06
120-Degree Capsule (EOC 19)	9	1.03	0.05
<b>Total Flux Wire Average</b>	<b>24</b>	<b>1.00</b>	<b>0.06</b>

## **5.2 Comparison of Predicted Activation to All BWR Plant Measurements**

Several BWR reactor units have had surveillance capsule activation analyses performed with the RAMA Fluence Methodology software. The results of several of these analyses have been previously documented [27]. Some additional analyses have been performed since then. The summary of all BWR analyses is presented in Table 5-8. The table contains the number of surveillance capsule measurements taken from all BWR plants. The comparison of those measurements to the calculated specific activities generated by RAMA (C/M) values is shown in

the last column of Table 5-8. The total C/M for all BWR capsules evaluated with RAMA is 0.99 with a standard deviation of  $\pm 9\%$ .

**Table 5-8  
Summary of BWR Operating Reactor Surveillance Capsule Measurement Comparisons**

Reactor Class	Fuel Assembly Configuration	No. of Samples	Calculated vs. Measured
BWR/2	560	317	0.98 $\pm 7\%$
BWR/3	484	18	1.03 $\pm 10\%$
BWR/3	400	6	1.09 $\pm 5\%$
BWR/4	368	27	1.04 $\pm 8\%$
BWR/4	548	18	0.93 $\pm 12\%$
BWR/4	560	39	1.00 $\pm 13\%$
BWR/4 & BWR/5	764	126	1.02 $\pm 9\%$
BWR/5	444	35	1.00 $\pm 9\%$
BWR/6	624	3	0.95 $\pm 1\%$
BWR/6	748	11	1.01 $\pm 9\%$
<b>Total</b>	---	<b>600</b>	<b>0.99 <math>\pm 9\%</math></b>

# 6

## REACTOR PRESSURE VESSEL FLUENCE UNCERTAINTY ANALYSIS

This section presents the combined uncertainty analysis and bias determination for the HC1 reactor pressure vessel fluence evaluation. The combined uncertainty is comprised of the comparison uncertainty factors developed in Section 5 and an analytic uncertainty factor developed in this section. When combined, these components provide a basis for determining the overall uncertainty ( $1\sigma$ ) and bias in the RPV fluence for this analysis.

The requirements for determining the combined uncertainty and bias for light water reactor fluence evaluations are provided in Regulatory Guide 1.190. The method implemented for determining the combined uncertainty and bias for reactor component fluence is described in the RAMA Theory Manual [1]. Regarding the determination of a bias in the fluence, Regulatory Guide 1.190 provides that an adjustment to the calculated fluence for bias effects is needed if a statistically significant bias exists in the fluence computation.

The results presented in this section show that the combined uncertainty for the HC1 RPV fluence evaluation is 9.9% and that no adjustment for bias effects is required to the calculated RPV fluence reported in Section 7 of this report.

The following subsections describe the comparison uncertainties determined in Section 5, the determination of the analytic uncertainty, and the determination of the overall combined uncertainty and bias for the HC1 RPV fluence evaluation.

### 6.1 Comparison Uncertainty

Comparison uncertainty factors are determined by comparing calculated activities with activity measurements. For pressure vessel fluence evaluations, two comparison uncertainty factors are considered: an operating reactor comparison uncertainty factor and a benchmark comparison uncertainty factor. The determination of a comparison uncertainty factor based on measurements involves the combination of two measurement components. One component is the variation in the comparison of the calculated-to-measured (C/M) activity ration and the other accounts for the uncertainty introduced by the measurement process.

### **6.1.1 Operating Reactor Comparison Uncertainty**

The operating reactor, or plant-specific, comparison uncertainty for the HC1 reactor is determined by combining the standard deviation for the activity comparisons with the measurement uncertainty for the plant-specific activity measurements.

### **6.1.2 Benchmark Comparison Uncertainty**

The benchmark comparison uncertainty used in the HC1 uncertainty analysis is based on a set of industry standard simulation benchmark comparisons.

## **6.2 Analytic Uncertainty**

The calculational models used for fluence analyses are comprised of numerous analytical parameters that have associated uncertainties in their values. The uncertainty in these parameters needs to be tested for its contribution to the overall fluence uncertainty.

The uncertainty values for the geometry parameters are based upon uncertainties in the dimensional data used to construct the plant geometry model. The uncertainty values for the material parameters are based upon uncertainties in the material densities for the water and nuclear fuel materials and the compositional makeup of typical steel materials. Since two sets of conflicting dimensional parameters are available for the surveillance capsule location, the dimensions which provided the most conservative uncertainty were used.

The uncertainty values for the fission source parameters are based upon uncertainties in the fuel exposure and power factors for the fuel assemblies loaded on the core periphery. The transport method used in the fluence analysis employs a fission source calculation that accounts for the relative contributions of the uranium and plutonium fissile isotopes in the fuel and the relative power density of the fuel in the reactor. Both fission source parameters are derived directly from information calculated by three-dimensional core simulator codes. The uncertainty values for the nuclear cross-section parameters are based upon uncertainties in the number densities for the predominant nuclides that make up the reactor materials.

The uncertainty parameters for the fluence model inputs are based upon geometry meshing and numerical integration parameters used in the neutron flux transport calculation. The process for determining the geometry meshing and numerical integration parameters involves an exhaustive sensitivity study that is described in the RAMA Procedures Manual [28].

## **6.3 Combined Uncertainty**

The combined uncertainty for the reactor pressure vessel fluence evaluation is determined with a weighting function that combines the analytic, plant-specific comparison, and benchmark

comparison uncertainty factors developed in Sections 6.1 and 6.2, above. Table 6-1 lists that the combined uncertainty ( $1\sigma$ ) determined for the HC1 reactor pressure vessel fluence is 9.9% for energy >1.0 MeV.

Table 6-1 also shows that, in accordance with Regulatory Guide 1.190, no bias term exists and it is not necessary to adjust the RAMA predicted RPV fluence in this analysis for bias effects. It is also demonstrated in Table 6-1 that the combined uncertainty is within the limits prescribed in U. S. NRC Regulatory Guide 1.190 (i.e.  $\leq 20\%$ ).

**Table 6-1**  
**HC1 RPV Uncertainty for Energy >1.0 MeV**

Uncertainty Term	Value
Combined Uncertainty ( $1\sigma$ )	9.9%
Bias	None <sup>(1)</sup>

- 1) The bias terms are less than their constituent uncertainty values, concluding that no statistically significant bias exists.

# 7

## CALCULATED REACTOR PRESSURE VESSEL NEUTRON FLUENCE FOR ENERGY >1.0 MEV

This section presents the predicted best-estimate fast neutron fluence (>1.0 <MeV) for the HC1 reactor pressure vessel (RPV) at EOC 19 (24.1 EFPY), and 56 EFPY. It is reported in Section 6 that the RAMA-calculated pressure vessel fluence for the HC1 reactor requires no bias adjustment; therefore, the best-estimate fluence is the calculated fluence that was predicted with the RAMA Fluence Methodology.

The reactor pressure vessel fluence reported in this section was determined at the interface of the RPV base metal and cladding, denoted as 0T location of the RPV wall as well as the 1/4 T and 3/4 T locations. The 1/4 T and 3/4 T depths are calculated based on the as-modeled RPV wall thickness of 15.50 cm (6.10 in). Reactor pressure vessel through-wall fast neutron fluence for use in embrittlement evaluations should be determined using an appropriate damage function (such as displacements per atom of iron) rather than the predicted fast neutron fluence obtained from transport calculations. Two acceptable methods for estimating the through-wall fluence are prescribed in U. S. NRC Regulatory Guide 1.99 [29]. A generic fluence attenuation formulation is provided for use when plant-specific damage assessments are not available and is given as:

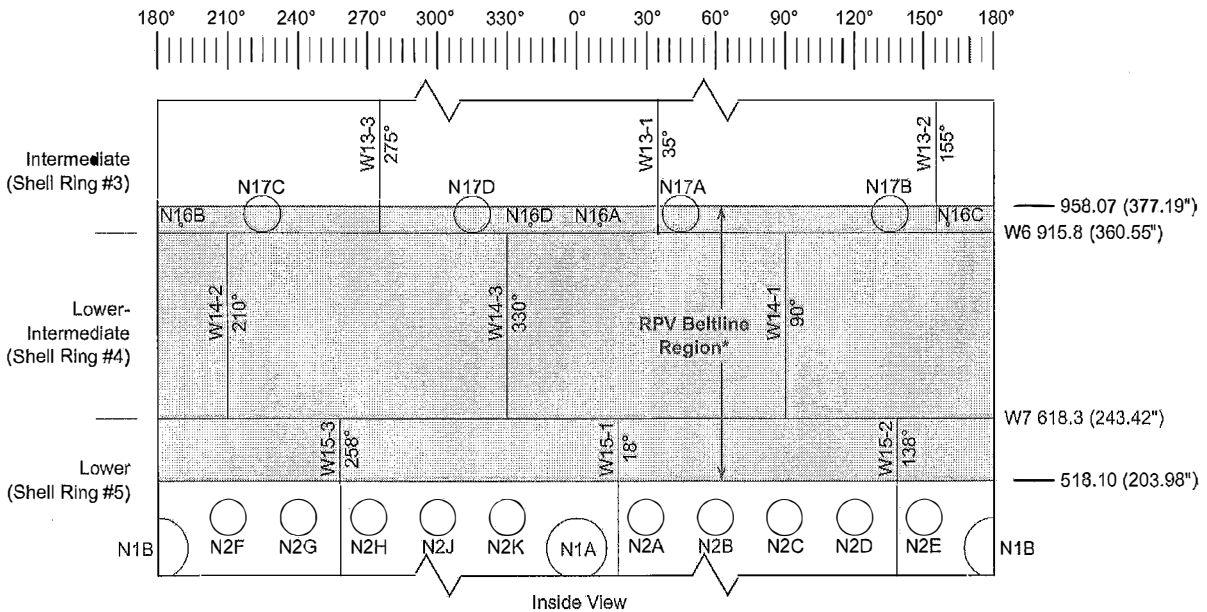
$$f_x = f_{surf} * e^{-0.24*x}$$

Where  $x$  is the depth in the RPV, given in inches, and  $f_{surf}$  is the fast neutron fluence at the vessel wetted surface. When plant-specific damage assessments are available, they may be used to obtain a more accurate estimate of the through-wall neutron fluence for embrittlement evaluations using the following formula:

$$f_x = f_{surf} * \frac{dpa_x}{dpa_{surf}}$$

Where  $dpa_x$  is the damage, expressed as displacements per atom of iron (dpa) at depth  $x$  and  $dpa_{surf}$  is the damage at the vessel wetted surface. HC1 plant-specific damage assessments are performed as a part of this fluence evaluation and are used to estimate the through-wall fluence, which is recommended for use in embrittlement evaluations.

The location and identification of the RPV plates, welds, and nozzles are shown in Figure 7-1. Also illustrated in Figure 7-1 is the calculated RPV beltline region for the HC1 reactor at 56 EFPY.



Notes: This drawing is not to scale.  
 Dimensions are given in centimeters (inches).  
 \* RPV beltline region is shown for 56 EFPY.

**Figure 7-1**  
**HC1 RPV Shell Plate, Weld and Nozzle Identifiers**

Fluence is presented for the RPV circumferential (girth) welds, vertical (axial) welds, nozzles, and plates residing in the RPV beltline region. Fluence in the RPV welds is presented at the center of the weld. Fluence for the nozzles is presented along two paths, one representing the nozzle forging-to-base-metal weld in the RPV shell course, the other representing the fluence along a 45-degree extraction path from the inside corner of the forging. Both paths are illustrated in Figure 7-2. Note that Figure 7-2 provides an example cutaway of the bottom half of a nozzle forging. The actual edit paths may occur at any orientation around the nozzle that coincides with the peak damage region. The OT and fractional depths are calculated based on the overall length of each respective path.

Table 7-1 reports the maximum fast neutron fluence at 0T, 1/4 T, and 3/4 T for the RPV circumferential and vertical welds in the RPV beltline region at EOC 19. Fluence values that exceed the threshold fluence of  $1.0E+17$  n/cm<sup>2</sup> are shown in **red**. The weld, plate, or nozzle with the highest fluence value in each table is shown in **bold** type. Table 7-2 reports the maximum fast neutron fluence for the RPV plates residing in the RPV beltline region at EOC 19. Table 7-3 reports the maximum fast neutron fluence for the RPV nozzles residing in the RPV beltline region at EOC 19. Table 7-4, Table 7-5, and Table 7-6 report the same fluence values as

Table 7-1, Table 7-2, and Table 7-3 respectively, but at 56 EFPY. Table 7-7 reports the elevations that define the RPV beltline at EOC 19 and 56 EFPY.

Note that all welds and plates, and the N16 and N17 nozzles exceed the threshold fluence of  $1.0E+17$  n/cm<sup>2</sup> at the inner surface prior to the end of cycle 19. The highest RPV fluence is reported for the lower-intermediate shell at 56 EFPY with a value of  $1.63E+18$  n/cm<sup>2</sup>.

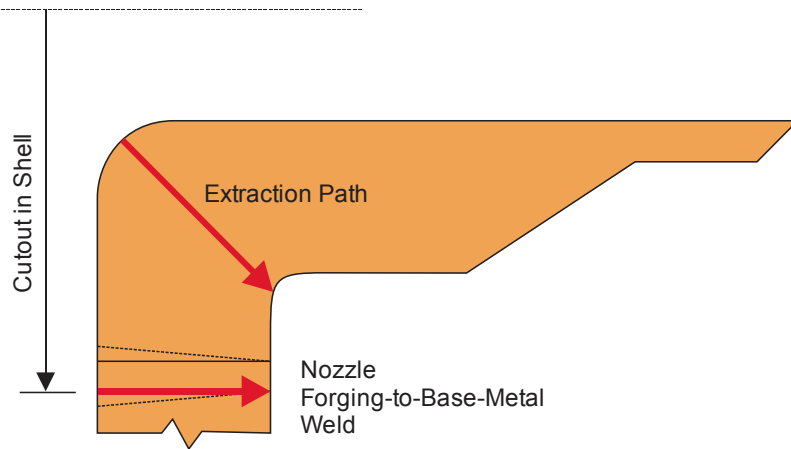


**Figure 7-2**  
**Nozzle Edit Locations for Sample Nozzle**

**Table 7-1  
Maximum Fast Neutron Fluence for HC1 RPV Beltline Weld Locations at EOC 19 (24.1 EFPY)**

Weld	Heat or Heat/Lot	Fast Neutron Fluence (n/cm <sup>2</sup> )		
		0T	1/4 T	3/4 T
<b>Intermediate Shell Axial</b>				
W13-1	510-01205 D53040/1125-02205	1.85E+17	1.32E+17	6.15E+16
W13-2		2.31E+17	1.63E+17	7.32E+16
W13-3		9.14E+16	6.62E+16	3.35E+16
<b>Lower-Intermediate Shell Axial</b>				
W14-1	510-01205 D53040/1125-02205	2.16E+17	1.56E+17	7.41E+16
W14-2		5.56E+17	3.89E+17	1.68E+17
W14-3		5.56E+17	3.89E+17	1.68E+17
<b>Lower Shell Axial</b>				
W15-1	510-01205 D53040/1125-02205	3.71E+17	2.59E+17	1.12E+17
W15-2		2.81E+17	1.98E+17	8.92E+16
W15-3		2.71E+17	1.91E+17	8.48E+16
<b>Shell Girth</b>				
W6	519-01205 504-01205 510-01205 D53040/1810-02205 D55733/1810-02205	2.35E+17	1.66E+17	7.44E+16
W7	501-01205 D53040/1125-02205	4.26E+17	2.97E+17	1.27E+17

**Table 7-2  
Maximum Fast Neutron Fluence for HC1 RPV Beltline Shell Plate Locations at EOC 19 (24.1 EFPY)**

Plate	Heat or Heat/Lot	Fast Neutron Fluence (n/cm <sup>2</sup> )		
		0T	1/4 T	3/4 T
<b>Intermediate Shell</b>				
3-1 3-2 3-3	5K3025/1 5K2608/1 5K2698/1	2.35E+17	1.66E+17	7.44E+16
<b>Lower-Intermediate Shell</b>				
4-1 4-2 4-3	5K2963/1 5K2530/1 5K3238/1	6.34E+17	4.39E+17	1.87E+17
<b>Lower Shell</b>				
5-1 5-2 5-3	5K3230/1 6C35/1 6C45/1	4.26E+17	2.97E+17	1.27E+17

**Table 7-3  
Maximum Fast Neutron Fluence for HC1 RPV Beltline Nozzle Locations at EOC 19 (24.1 EFPY)**

Nozzle Location	Heat or Heat/Lot	Fast Neutron Fluence (n/cm <sup>2</sup> )		
		0T	1/4 T	3/4 T
N2 Weld	N/A	1.35E+16	1.15E+16	9.11E+15
N2 Extraction Path	N/A	1.99E+15	2.40E+15	5.09E+15
N16 Weld	N/A	1.51E+17	1.09E+17	5.23E+16
N16 Extraction Path	N/A	1.41E+17	1.18E+17	6.88E+16
N17 Weld	001-01205 519-01205 504-01205	2.09E+17	1.57E+17	7.45E+16
N17 Extraction Path	19468/1 10024/1	7.40E+16	6.08E+16	4.58E+16

**Table 7-4  
Maximum Fast Neutron Fluence for HC1 RPV Beltline Weld Locations at 56 EPY**

Weld	Heat or Heat/Lot	Fast Neutron Fluence (n/cm <sup>2</sup> )		
		0T	1/4 T	3/4 T
<b>Intermediate Shell Axial</b>				
W13-1	510-01205 D53040/1125-02205	4.32E+17	3.09E+17	1.45E+17
W13-2		5.50E+17	3.89E+17	1.75E+17
W13-3		2.16E+17	1.57E+17	7.99E+16
<b>Lower-Intermediate Shell Axial</b>				
W14-1	510-01205 D53040/1125-02205	5.56E+17	4.01E+17	1.90E+17
W14-2		1.43E+18	1.00E+18	4.34E+17
W14-3		1.43E+18	1.00E+18	4.34E+17
<b>Lower Shell Axial</b>				
W15-1	510-01205 D53040/1125-02205	1.00E+18	6.97E+17	3.01E+17
W15-2		7.00E+17	4.95E+17	2.24E+17
W15-3		7.20E+17	5.07E+17	2.25E+17
<b>Shell Girth</b>				
W6	519-01205 504-01205 510-01205 D53040/1810-02205 D55733/1810-02205	5.55E+17	3.94E+17	1.77E+17
W7	501-01205 D53040/1125-02205	1.15E+18	8.02E+17	3.42E+17

**Table 7-5  
Maximum Fast Neutron Fluence for HC1 RPV Beltline Shell Plate Locations at 56 EFPY**

Plate	Heat or Heat/Lot	Fast Neutron Fluence (n/cm <sup>2</sup> )		
		0T	1/4 T	3/4 T
<b>Intermediate Shell</b>				
3-1	5K3025/1	5.55E+17	3.94E+17	1.77E+17
3-2	5K2608/1			
3-3	5K2698/1			
<b>Lower-Intermediate Shell</b>				
4-1	5K2963/1	1.63E+18	1.14E+18	4.84E+17
4-2	5K2530/1			
4-3	5K3238/1			
<b>Lower Shell</b>				
5-1	5K3230/1	1.15E+18	8.02E+17	3.42E+17
5-2	6C35/1			
5-3	6C45/1			

**Table 7-6  
Maximum Fast Neutron Fluence for HC1 RPV Beltline Nozzle Locations at 56 EFPY**

Nozzle Location	Heat or Heat/Lot	Fast Neutron Fluence (n/cm <sup>2</sup> )		
		0T	1/4 T	3/4 T
N2 Weld	N/A	3.74E+16	3.17E+16	2.46E+16
N2 Extraction Path	N/A	5.55E+15	6.61E+15	1.37E+16
N16 Weld	N/A	3.58E+17	2.59E+17	1.25E+17
N16 Extraction Path	N/A	3.34E+17	2.81E+17	1.65E+17
N17 Weld	001-01205 519-01205 504-01205	4.81E+17	3.62E+17	1.73E+17
N17 Extraction Path	19468/1 10024/1	1.69E+17	1.39E+17	1.06E+17

**Table 7-7**  
**Reactor Beltline Elevation Range for HC1 for Energy >1.0 MeV**

Reactor Lifetime	Lower Elevation [cm (in)]	Upper Elevation [cm (in)]
EOC 19 (24.1 EFPY)	541.78 (213.30)	937.92 (369.26)
56 EFPY	518.10 (203.98)	958.07 (377.19)

# 8

## REFERENCES

1. BWRVIP-114-A: BWR Vessel and Internals Project, *RAMA Fluence Methodology Theory Manual*, EPRI, Palo Alto, CA: 2009. 1019049.
2. Letter from William H. Bateman (U. S. NRC) to Bill Eaton (BWRVIP), “Safety Evaluation of Proprietary EPRI Reports BWRVIP-114, -115, -117, and -121 and TWE-PSE-001-R-001,” dated May 13, 2005.
3. Letter from Matthew A. Mitchell (U. S. NRC) to Rick Libra (BWRVIP), “Safety Evaluation of Proprietary EPRI Report BWR Vessel and Internals Project, Evaluation of Susquehanna Unit 2 Top Guide and Core Shroud Material Samples Using RAMA Fluence Methodology (BWRVIP-145),” dated February 7, 2008.
4. “Safety Evaluation Report with Open Items Related to the License Renewal of Seabrook Station,” Docket Number 50-443, dated June 2012.
5. “Calculational and Dosimetry Methods for Determining Pressure Vessel Neutron Fluence,” Nuclear Regulatory Commission Regulatory Guide 1.190, March 2001.
6. Code of Federal Regulations, Title 10, Part 50, Appendix B, “Quality Assurance Criteria for Nuclear Power Plants and Fuel Reprocessing Plants,” Aug. 28, 2007.
7. Code of Federal Regulations, Title 10, Part 50, Appendix G, “Fracture Toughness Requirements,” Dec. 12, 2013.
8. Code of Federal Regulations, Title 10, Part 50, Appendix H, “Reactor Vessel Material Surveillance Program Requirements,” Jan. 31, 2008
9. “Transmittal of Hope Creek Cycle 1 through 12 Processed POCLA4 Data from HCP.6-0209 and Fuel Design Data from HCP.6-0213,” letter from D. V. Notigan (PSEG) to D. B. Jones (TWE), 12/21/2005.
10. “Transmittal of Hope Creek Cycle 6 through 12 P11 Data from HCP.6-0211,” letter from D. V. Notigan (PSEG) to D. B. Jones (TWE), 12/21/2005.
11. “Transmittal of Supporting Files for Design Analysis 80093291-0020-0001, Hope Creek Fluence Operating Data for Cycles 13, 14, and EPU,” transmittal number 80093291-0020-0003, Don Notigan (PSEG) to Dean Jones (TWE), 3/13/08.
12. “HC ISP Fluence Inputs for Cycles 15-19,” PSEG Nuclear Fuels BWR Design and Analysis, HCP.6-0285, Rev. 0.
13. “Hope Creek Cycle 1 to 12 Core Weights and Effective Full Power Days,” PSE&G Report HCP.6-0210, December 01, 2005.
14. “Fuel and Operating History Data for Cycles 13, 14, and 3840 MWt EPU to Support Hope Creek Unit 1 Fluence Analysis,” PSEG report 80093291-0020-0001, Rev. 0.
15. “Cycle 15 and 16,” email from Frank Saffin (PSEG) to Eric Jones (TWE), 6/1/2015.

16. "Cycle 17, 18, 19," email from Frank Saffin (PSEG) to Eric Jones (TWE), 6/1/2015.
17. "Transmittal of HC Mechanical Design Drawings in Support of Shroud Fluence Project PSE-FLU-001," Transmittal from Don Notigan of PSEG to Dean Jones of TransWare Enterprises Inc, 12/2/2005.
18. "Transmittal of Design Information," To Dean Jones, From Randy Schmidt. Transmittal Number 80093291-0020-0011. 4/28/2008.
19. GE Hope Creek Capsule Dimensions, GE Document GE-NE-0000-0016-8305, Rev. 0.
20. "Licensing Version of Hope Creek Generating Reactor Pressure Vessel Fluence Evaluation at 56 EFPY," TransWare Enterprises Inc., PSE-FLU-002-R-003, Rev. 0, August 2008.
21. "Fluence Evaluation for Hope Creek Generating Station 120-Degree Surveillance Capsule Using RAMA Fluence Methodology," TransWare Enterprises Inc., EPR-HC1-001-R-001, Rev. 0, March 2016.
22. "BUGLE-96: Coupled 47 Neutron, 20 Gamma-Ray Group Cross Section Library Derived from ENDF/B-VI for LWR Shielding and Pressure Vessel Dosimetry Applications," RSICC Data Library Collection, DL2C-185, March 1996.
23. "VITAMIN-B6: A Fine-Group Cross Section Library Based on ENDF/B-VI Release 3 for Radiation Transport Applications," RSICC Data Library Collection, DLC-184, December 1996.
24. "Determination of Fast Neutron Flux Density and Fluence: Hope Creek Generating Station," General Electric Company, WA KTZ903595, February 23, 1989.
25. "Hope Creek 1 Generating Station RPV Surveillance Materials Testing and Fracture Toughness Analysis," General Electric Company, GE-NE-523-A164-1294, Rev. 1, December 1997.
26. "Testing and Evaluation of the Hope Creek 120 Degree Surveillance Capsule," MP Machinery & Testing, LLC, MPM-23016, March 2016.
27. BWRVIP-189: BWR Vessel and Internals Project, *Evaluation of RAMA Fluence Methodology Calculation Uncertainty*, EPRI, Palo Alto, CA: 2008. 1016938.
28. BWRVIP-121-A: BWR Vessel and Internals Project, *RAMA Fluence Methodology Procedures Manual*, EPRI, Palo Alto, CA: 2009. 1019052.
29. "Radiation Embrittlement of Reactor Vessel Materials," Nuclear Regulatory Commission Regulatory Guide 1.99, Revision 2, 1988.